NANOXSOLAR

A division of NXS Technologies, Inc.

"INNOVATION IN SOLAR FOR A BRIGHT FUTURE!"

SOLAR WAFER TECHNOLOGY

WHITE PAPER

Standardizing our Panel-wafer white paper

As we pull a fresh ingot off the crystal puller, the current new wave of wafers are 210-220mm size ingot. A spindle weighting hundred of lbs, is sent to the processing room for Diamond wire sawing. Over the years the wafer thickness has went into development. Slicing differences in 150 microns to 210 microns allowed for photovoltaic changes in module efficiency and greater ranges when designing a new panel.

Thickness Statistics

Once we open the doors 100% production of NanoXSolar Mono-crystalline wafers had entered cutting with diamond wire. After 2 years of technology research and development, the 110µm wafer technology has been developed. Except mass production of 180µm, 170µm and 160µm, samples of all thicknesses can be made and mass production can be available in 2-4 months. As we follow the trend with high energy lasers, we can develop processing wafers with laser cutting cleaving and automated processing with no waist.

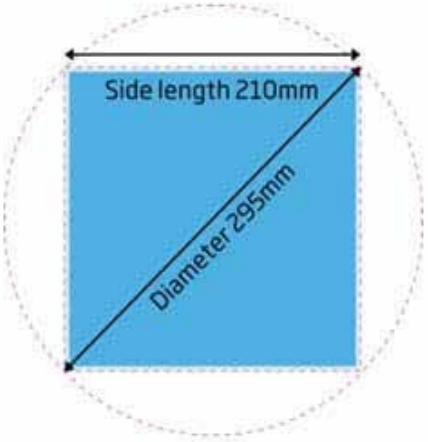

210-1: Size 440.96cm^2

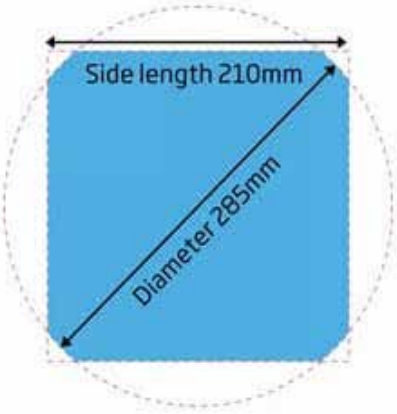

210-2: Size 439.55cm^2

NANOXSOLAR
A division of IIX5 Technologies, Inc.

Standardizing our
Panel-wafer white paper

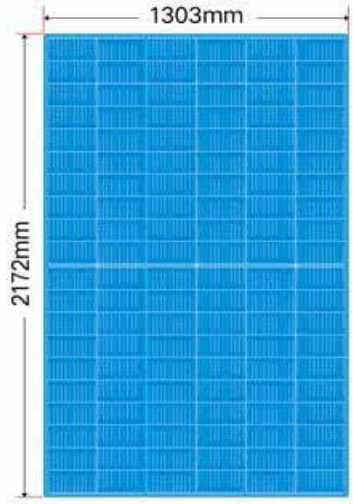

120 Half cell

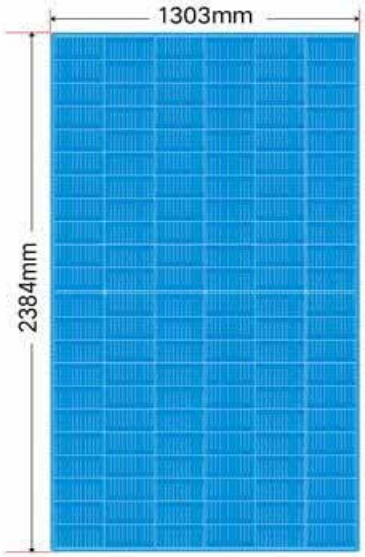

132 Half cell

210mm (Next-Gen), 182mm (Current-Gen) module, 158mm-166mm (Legacy) "Sun-power/Longi"

210mm and 182mm cells have the same PERC structure and their efficiency is almost the same. By theory bigger wafers are not necessarily better, they help reduce the overhead cost with logistics. Single next-Gen panels to achieve 800-1000W per module.

Total cost calculation of large-size products value chain			
	182(535W) VS 166(445W)	210(545W) VS 166(445W)	210(545W) VS 182(535W)
Silicon material	0.0009	0.0011	0.0002
Non-silicon cost of silicon	-0.0278	-0.0473	-0.0195
Silicon wafer (=Silicon material + Non-silicon cost)	-0.0269	-0.0462	-0.0193
Non-silicon cost of cell	-0.0188	-0.0321	-0.0134
Cell (Silicon wafer + Non-silicon cost of cell)	-0.0457	-0.0784	-0.0327
Non-silicon cost of module	-0.0247	-0.0279	-0.0032
Module (Cell + Non-silicon cost of module)	-0.0704	-0.0462	-0.0359
BOS	-0.0291	-0.0745	-0.0454
Power station system(module + BOS)	-0.0995	-0.1808	-0.0813
Logistics	-0.0089	-0.0102	-0.0013
Total cost of value chain (power station system + Logistic)	-0.1084	-0.1910	-0.0826

Standardizing our Panel-wafer white paper

The increase in current in the 210mm ultra-high-power module is driven by a larger cell, as current is the product of current density multiplied by cell area.

In addition, for the same module efficiency, the amount of unutilized heat – the solar energy which cannot be converted into electric energy – is the same in terms of unit area. Integration of sputtering and no-facial PERC wafers with nano materials ie Diamond, DLC-Diamond Like Carbon, Carbon Nano-tubes and customized backing flex cell IC will allow us to advance with temperature stability with increased size in wafers from the standard M10/M12 144-168mm standard size from Sunpower/Longi. They tend to use a legacy wafer size that they feel is not needing the push towards a larger ingot size for next-Generation product development.

As a module's operating temperature rises, the open-circuit voltage will decrease, while the short-circuit current increases slightly, leading to decreases in photovoltaic conversion efficiency and cell power. According to the company study, an energy loss of 0.20% occurs for every 1 of increase in operating temperature.

The integrated use of R&D processes, nano technologies with multi-heterojunction cells will allow the refractive light to capture the most efficiently conversion of light without the use of solar trackers. The multi-layer cell can capture RGB bands of light to increase cell production with adding perovskites into the production process to spray metal halide lead bases film, then a process with a 5kW microwave oven bakes the inkjet style printing into glass.This goes thru some final processes to complete the layers, sputtering and quality control to complete the junction wafer processing of wafer on our assembly line for increased production rate of dropping module cost per watt adoption.

Wafer size development over the years - https://en.longi-silicon.com/index.php?m=-content&c=index&a=lists&catid=90

USPTO patents to be obtained on utility designs of equipment, processing improves and nano material adoption. We are working with Blue Wave Semi, Oxford PV, and Ben at Solarinnovations "2020 Patent wafer of the year" to continue our R&D efforts with leaders in the industry. As we open our doors, build our team, stage our foundry and continue to achieve on breaking the laws of physics. We only want the best talented engineers, chemist, and material scientists at NanoXSolar.

Introduction
Our Mother Company

Mitsuboshi Diamond Industrial Co., Ltd.Japanese manufacturer for glass cutting machines and toolsmainly for FPD market, established 1935

The company Mitsuboshi Diamond in the 1950's

New factory in Iida / Japan

Content

Cutting of Glass- History

In the Middle Ages glass was cut with a heated and sharply pointed rod of iron. The red hot point was drawn along themoistened surface of the glass causingit to snap apart. Fractures created in this way were notvery accurate. Rough pieces had to bechipped or "grozed" down to more exact shapes with a hooked tool called “grozingiron”.

In 1869 the wheel cutter was developedby Samuel Monce of Bristol, Connecticut,which remains the current standardtool for manual glass cutting.

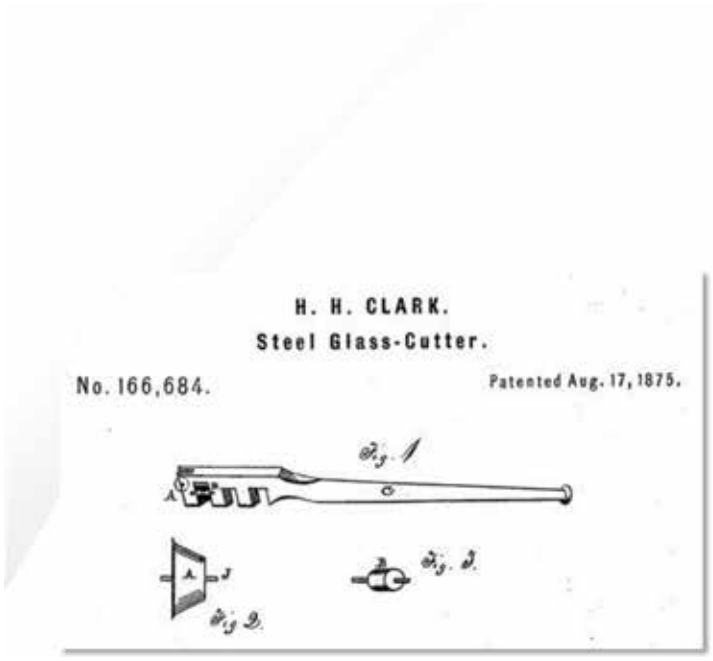
H. H. CLARK.
Steel Glass-Cutter.
No. 166,684. Patented Aug. 17, 1875.

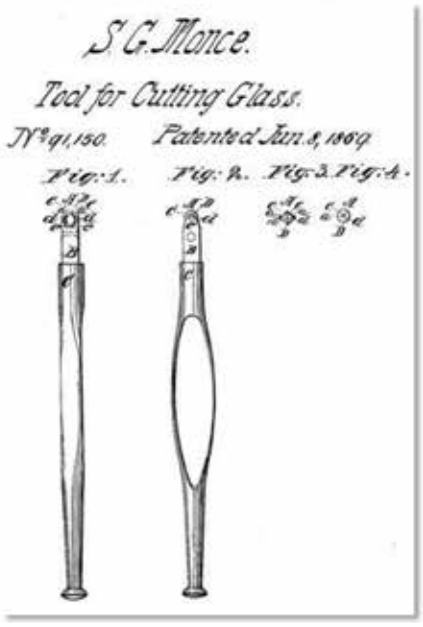
S. G. Monce.
Tool for Cutting Glass.
Patented Jun. 8, 1869.

NANOXSOLAR
A division of NXS Technologies, Inc.

Cutting of Glass – Tools

Manual

Normal Cutting Wheels Structured Cutting Wheels Holders and Axles

http://www.nanoxsolar.com/

Cutting of Glass

If you take a piece of glass and try to break it without first scribing it, it will seem quite strong and will resist breaking. It will bend a little, because the force you are applying is evenly applied all over the glass.

Hitting the glass by mechanical force causes tensions of > 500MPa but it will not break if there are no cracks or damages at the edge.

You will have no control over where it breaks, exactly when it breaks, what the shape of the break will be, or how many pieces it will break into. You will probably cut yourself as well.

However, if you scribe the glass first, it will be weaker than before, because you generate micro cracks and other damages along the scribed line.

A scribe line, if left alone long enough, will begin to “repair” itself and close again. In order to avoid the healing, a cutting liquid may be helpful.

The glass is now stressed at that point, and it will take little external pressure to cause it to separate along the scribe line.

As a result, it will break along the scribe line with considerably less force than it was needed to break an unscored piece of glass e.g. when breaking by hand.

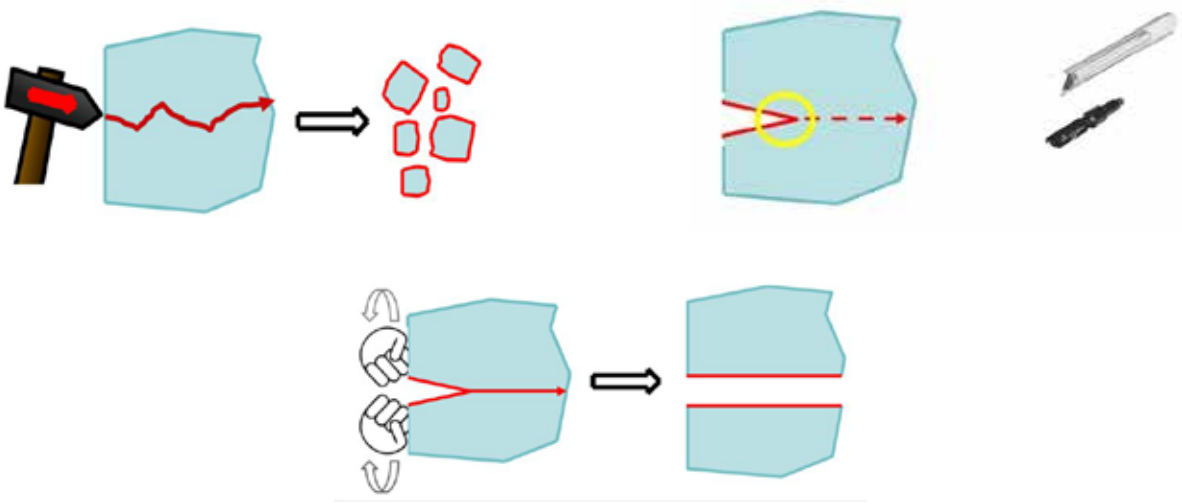

Evaluation of Glass Cut

How to evaluate a glass cut ?

Beside investment and running costs there are three important points to consider when evaluating a glass cut:

Point 1 – Edge strength:

For most of the final applications a proper edge strength is a must and the glass should not break easily

Point 2 – Chippings:

Often chipping is not allowed or should be minimized whereas Cleaning is expensive

Point 3 – Post processing:

After cutting the glass following processing methods like grinding or polishing are required.Cutting has to be adjusted to the whole process line

Evaluation of Glass Cut

Edge strength of glass

Statistical evaluation (> 35 samples at least)

- A sample is stressed until it breaks
- The force / tension needed to break is measured
- Often a Weibull function is used to display

There are several methods in industry to measure the glass strength. Most common tests are:

1. 4 Point Bending: evaluates the strength of the glass edge
2. Ring to Ring: evaluates overall strength of a glass piece
3. Ball Drop: evaluates overall strength of a glass piece

Evaluation of Glass Cut-Methods

4 Point Bending

A Sample is placed on two supporting pins a set distance apart. Two loading pins placed at an equal distance around the center are lowered from above at a constant rate until sample failure.

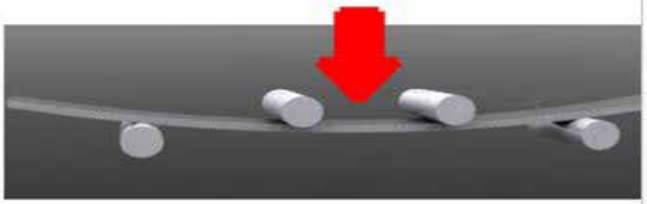

Advantage:

constant flexural stress between the two supporting pins.

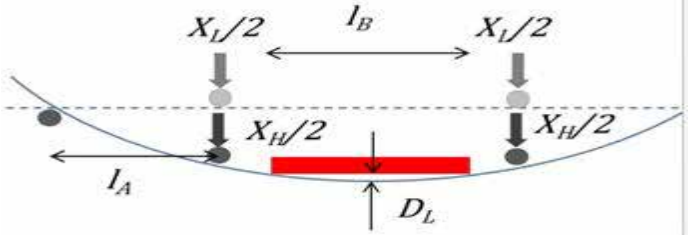

Source: Wikipedia

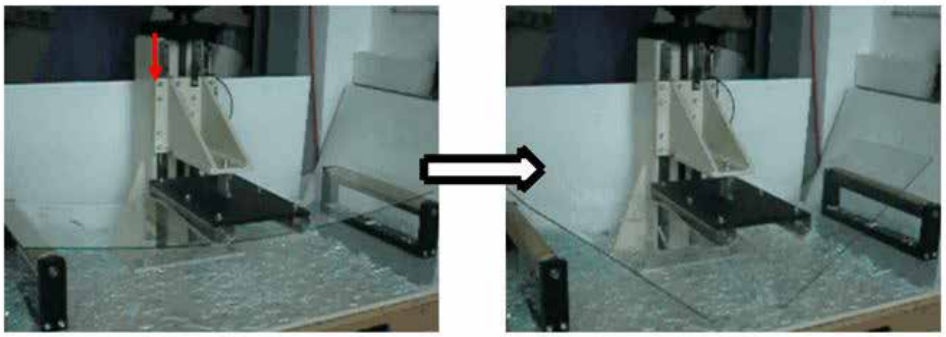

Wheel Cut

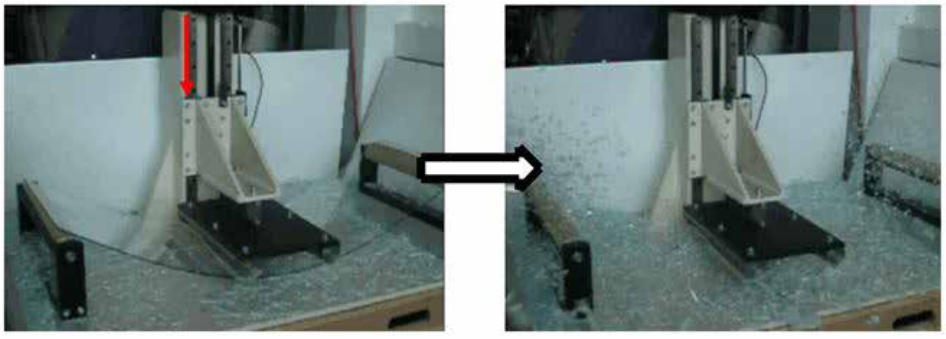

laser Cut

Evaluation of Glass Cut-Methods

Ring to Ring Test

Glass substrate or panel is placed on a ring. A smaller loading ring is placed at an equal distance around the center is lowered from above at a constant rate until sample failure.

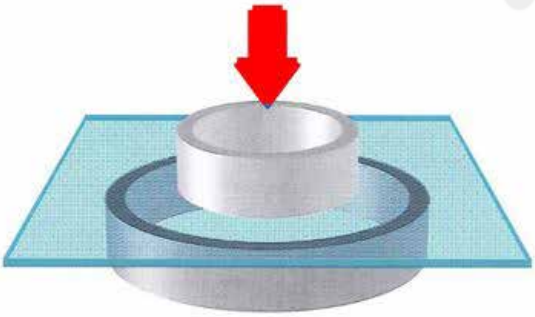

Tests primary surfaces but not edges; highest stress at loading ring

Continuous stress increase

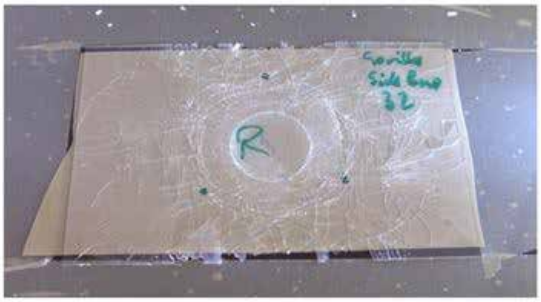

Advantage:

simple test setup

Ball Drop Test

This method evaluates the height where the glass breaks by dropping a stainless steel ball on the sample.

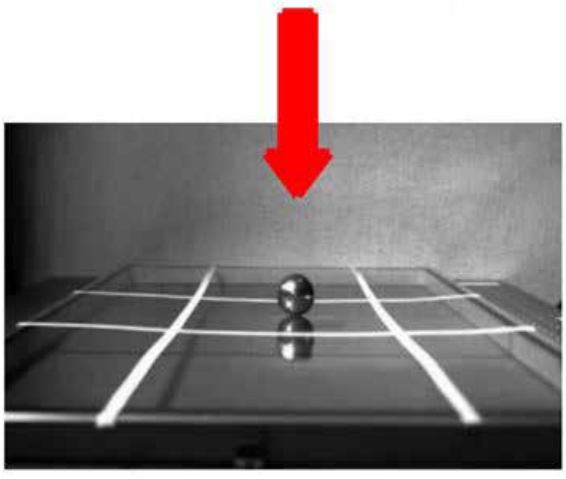

Cutting with Wheels – The Process

The Scribing Process

A cutting wheel, made of tungsten carbide or polycrystalline diamond and with a V-shaped profile, is pressed firmly against the surface of the glass and a line is briskly scribed to form a "score" or "cut".

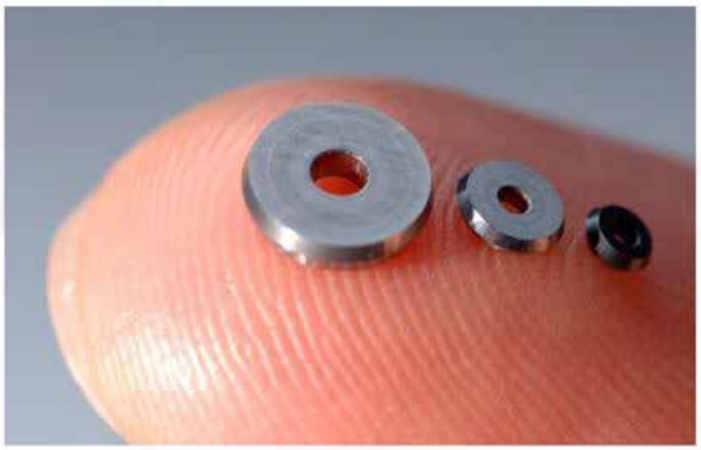

The Breaking Process

The glass is now weakened along the scribe line and the glass sheet is ready to be “broken” in two.

Cutting with Wheels – Scribe & Break

STEP1

Scribing

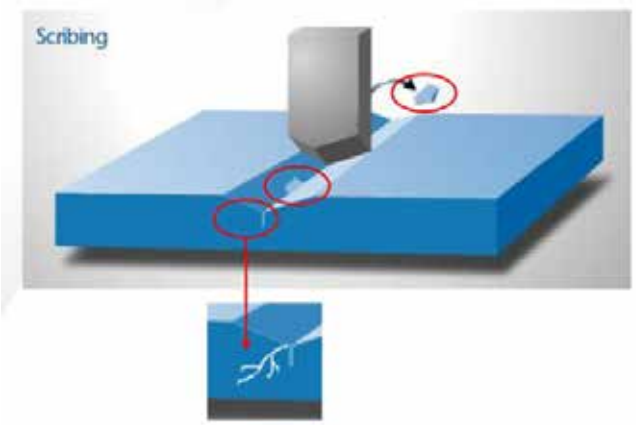

Disadvantages

- Broken out glass fragments and chip-pings
- Micro cracks
- Fragments left in cut path > Edge chips
- The cut is not perpendicular to glass

STEP2

Breaking

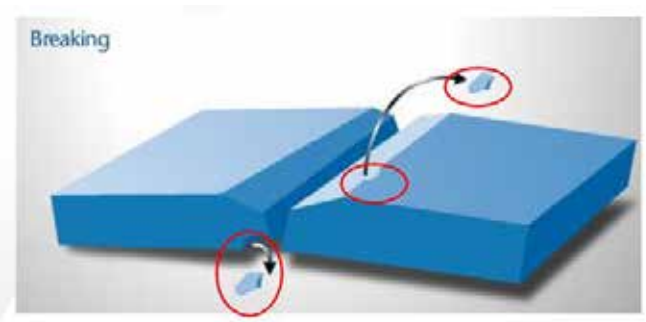

Disadvantages

- Fragmentation on the under side of glass
- Break is not occurring along cut path
- necessity of second step is costly and time-consuming

Cutting with Wheels – Products

Depending on glass thickness (t), according wheel angles (V) should be used.

Example:

Diamond pin / wheel	t = 50µm to 200µm	V = 105˚or 110˚
Diamond wheel	t ≥ 200µm	V = 110˚
Diamond wheel	t ≥ 400µm	V = 110˚or 115˚
Carbide wheel	t ≥ 600µm	V = 115˚or 120˚

Cutting tool by Mitsuboshi

Cutting tool by Bohle

Diamond pin by Lach

NANOXSOLAR
A division of IXS Technologies, Inc.

Cutting with Wheels – Machines

Automatic float glass cutting machine

State-of-the-Art technology with magnetic linear drives

Laminated glass cutting machine

Cutting of laminated glass and float glass for maximum work-load and flexibility

Glass processing line

High performance in glass cutting and handling

http://www.nanoxsolar.com/

Cutting with Wheels – Penett®

Breakthrough in FPD market

Due to the demands in consumer electronics, glass was getting thinner and handling got a bigger importance

To overcome disadvantages of normal wheel cutting, the development of structured wheels started in the 1990th

Targets:

Simplify or even eliminate no breaking process & Increase edge strength

A new technology

The deep penetration cutting wheel was invented in 1998 by MDI; breakless separation of FPD (Flat Panel Displays) became possible

Consecutive hitting caused by the unique wheel structure (notches) creates very deep median cracks up to 90% of the glass thickness

Conventional cutting wheel

Penett® cutting wheel by MDI

NANOXSOLAR
A division of IXS Technologies, Inc.

Cutting with Wheels – Penett®

Comparison: conventional wheel cut vs. Penett® wheel cut

Essential advantages of deep penetration cutting wheels such as Penett®:

- No lateral cracks
- Median cracks depth up to 90% enables
- easy breaking process

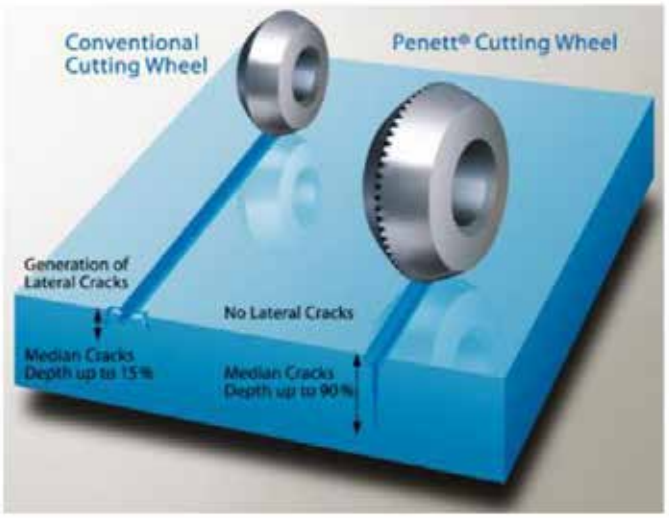

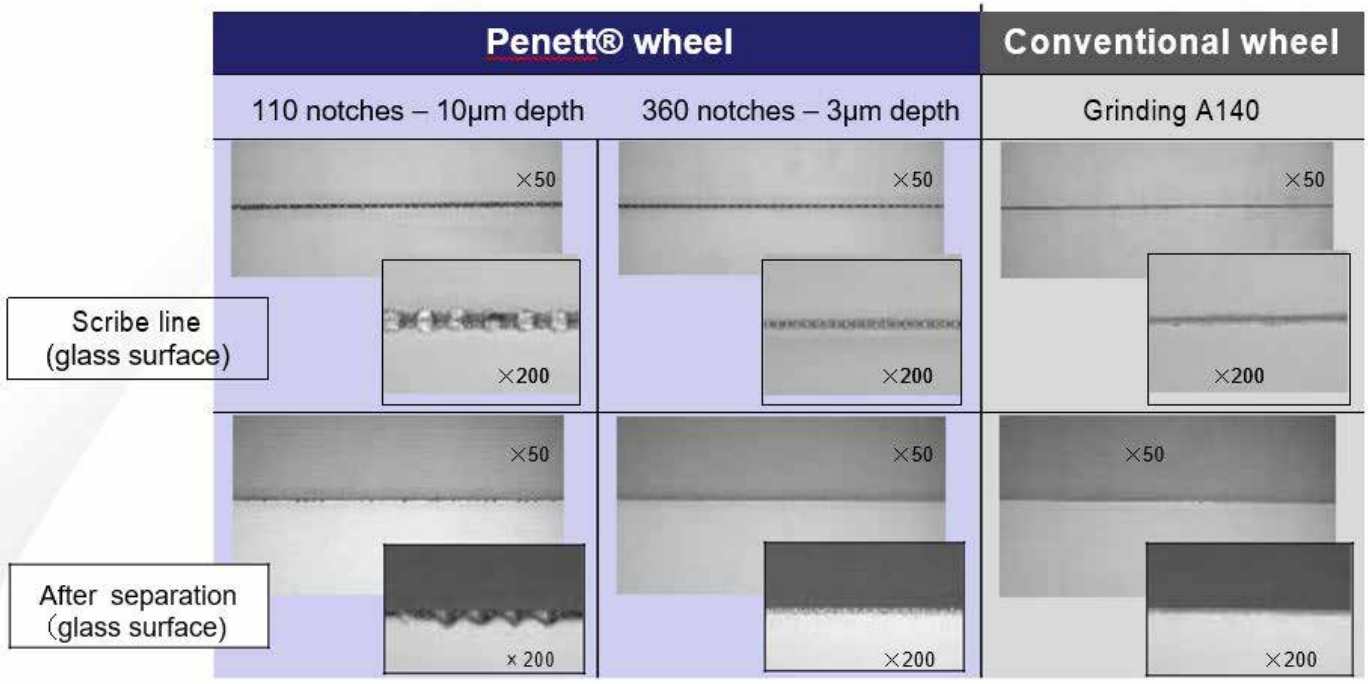

http://www.nanoxsolar.com/

Cutting with Wheels – Penett®

Weibull distribution

Edge strength comparison: conventional wheel cut vs. Penett® wheel cut

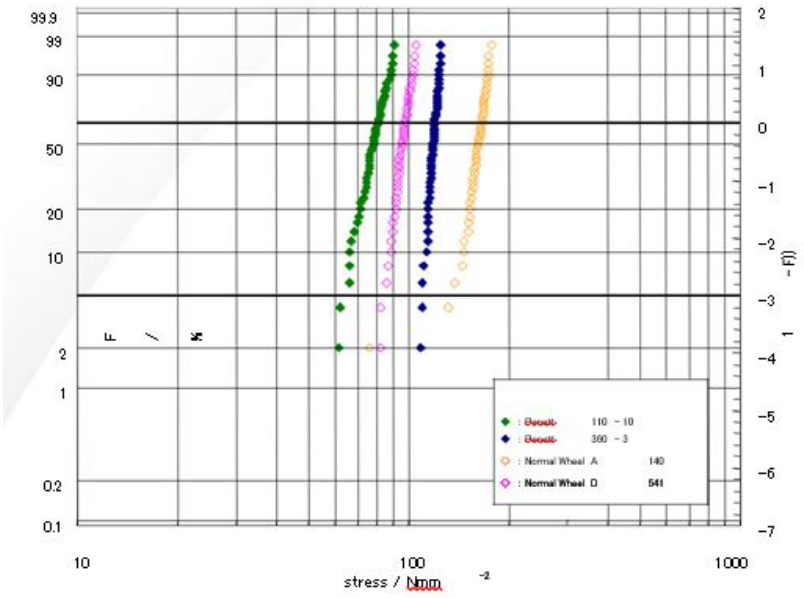

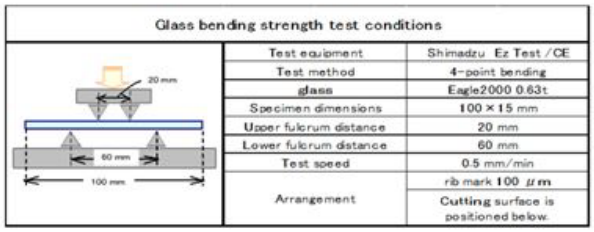

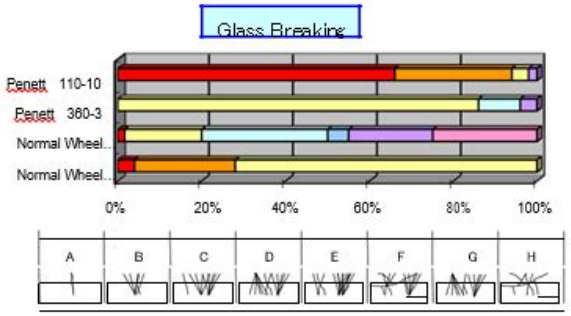

NANOXSOLAR
A division of NXS Technologies, Inc.

Cutting with Wheels – Machines

Automatic glass scriber

MS Series with single cutting head

MM Series with multiple cutting heads

Inline glass separation systems

Separation of super-large liquid-crystal panels.Simultaneous separation of both upper and lower side of panels

http://www.nanoxsolar.com/

Cutting with CO2 Laser

Advancements in laser technology opened new doors

Structured wheels improve breakability of glass, but no improvement regarding edge strength and chipping

To overcome disadvantages of Penett wheels, CO2 laser technology entered glass production in year 2000

Targets:

increase cutting edge strength (especially cell phones, later on touch panels for smartphones)
reduce or even eliminate chippings

Principle of thermal stress cutting – a contactless process

Focused laser beam heats up a specific line on the glass, followed by a cold jet of air / liquid mixture from cooling nozzle

This thermally induced tension causes precise fissuring of glass

Advantages:

- No further processing like grinding or polishing needed
- No micro cracks / chipping
- No material loss
- For cleanroom applications

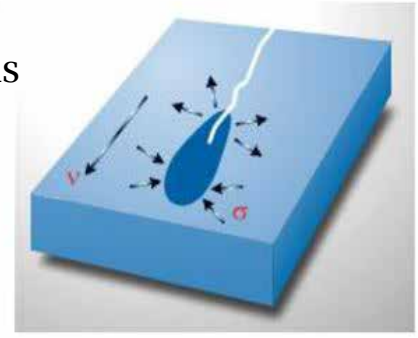

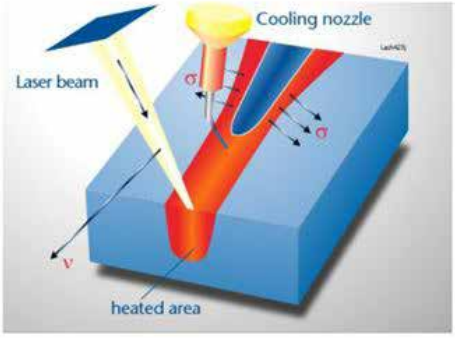

Cutting with CO2 Laser

Comparison: conventional wheel cut vs. laser cut

Glass D263, thickness t=0.4mm

Laser full cut or laser scribe

Laser full cut: completely cuts the glass using only laser process & requires a further breaking process for separation

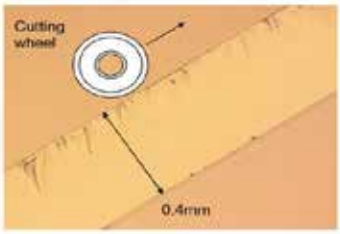

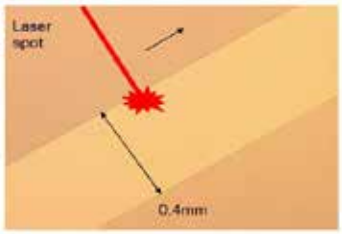

Weibull distribution

Edge strength comparison: wheel cut (conventional and Penett®) vs. CO2 cut

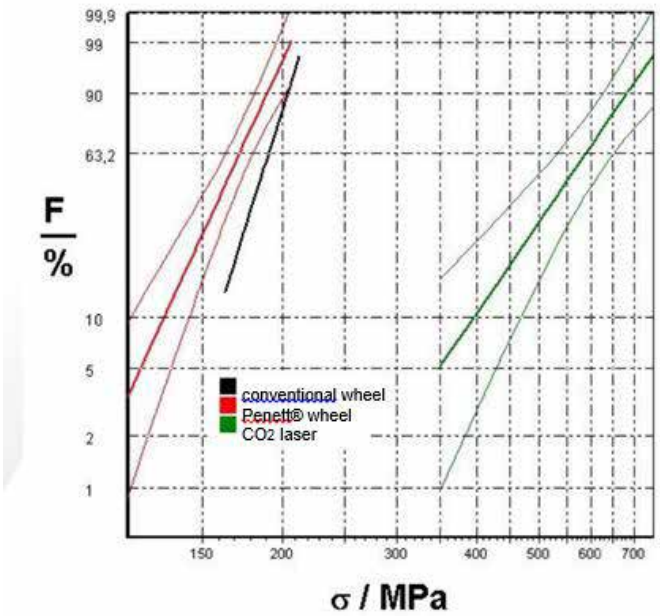

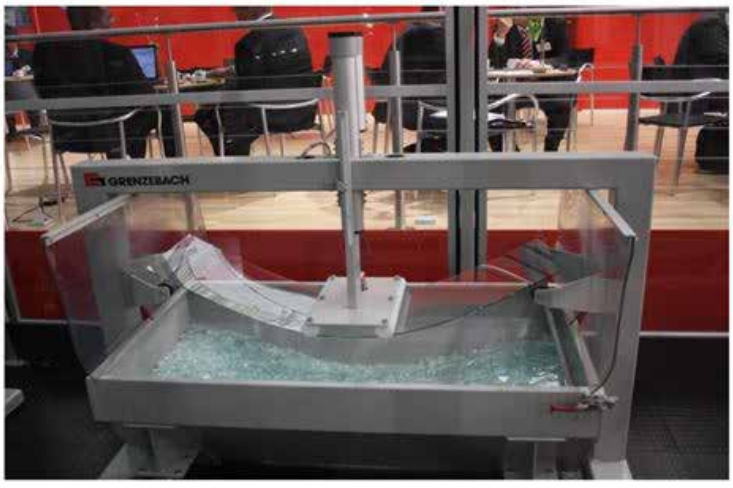

Source: Grenzebach GmbH

Cutting of ultra thin glass (thickness 30 – 300µm)

Highest edge strength due to cutting by CO2 laser without micro cracks

Cutting with CO2 Laser-Machine

TGC Series (Thin Glass Cutter)

- High edge strength up to 1000MPA
- Glass bendable up to r = 2mm
- Laser cut enables easy handling
- Special beam guiding also for
- free shape cutting

TGC1350

Cutting by Ablation

Next step: laser shape cutting

- CO2 Laser cutting improves glass edge strength and reduces chippings, limitation in free shape cutting
- Around 10 years ago the question popped up how to cut out shapes inside the glass without destroying it

Source: SCHOTT AG

Target:

- cutting of flexible shapes
- cutting out shapes inside the glass using laser technology

Micro processing by green laser (532nm) or UV laser

Drilling, grooving, marking, patterning and coating

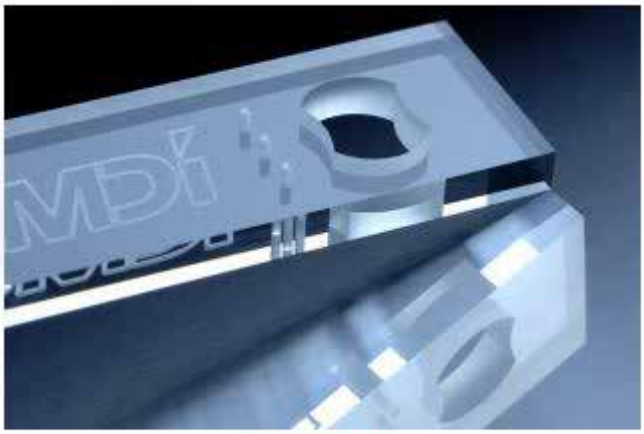

Company logo in glass

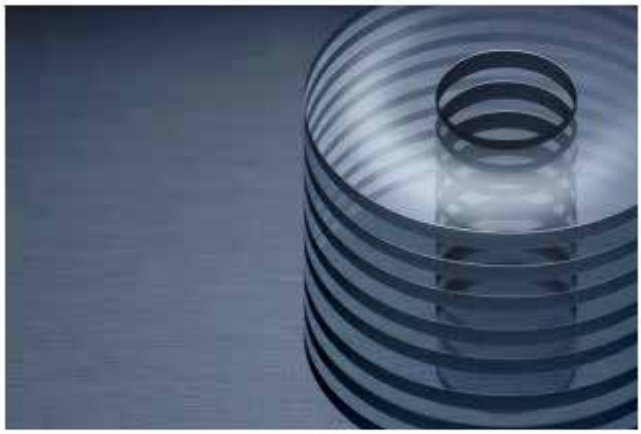

Encoder Disks

Cutting by Ablation-Drilling

Drilling with green laser technology

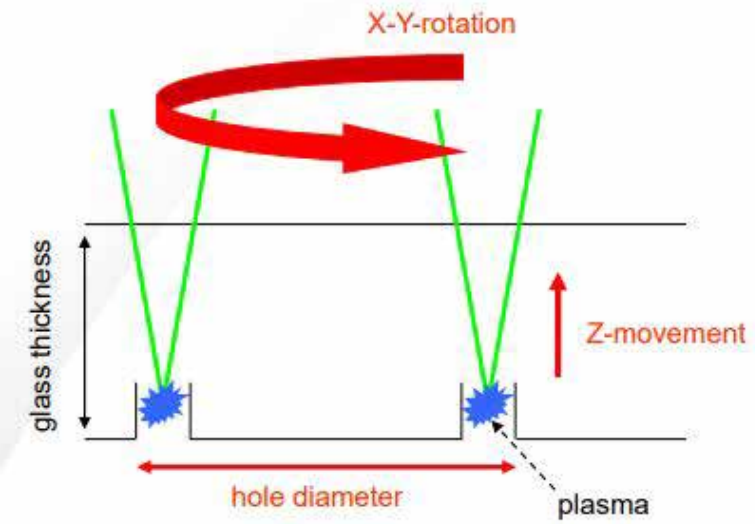

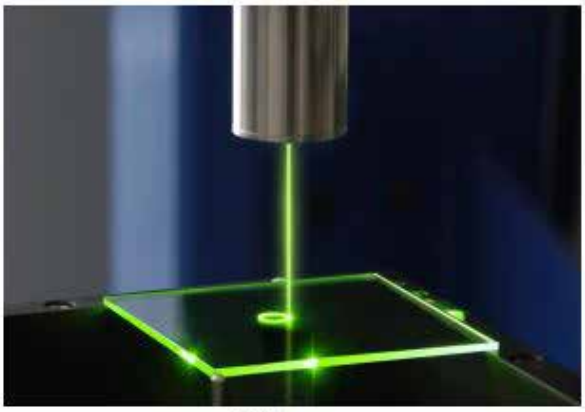

Drilling process

Cutting by Ablation-Chamfering

Chamfering with green laser technology:Green laser processing enables edge chamfering on the opposite side of the optic device

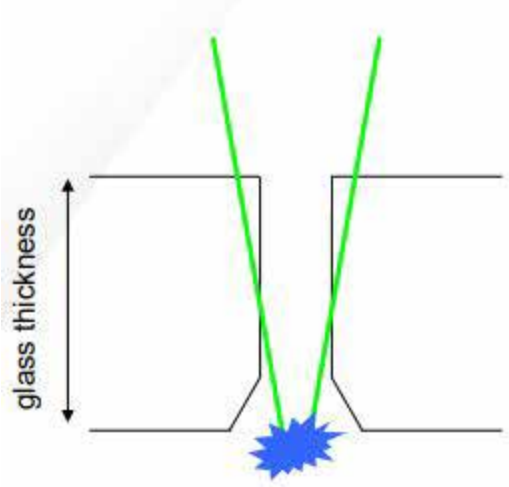

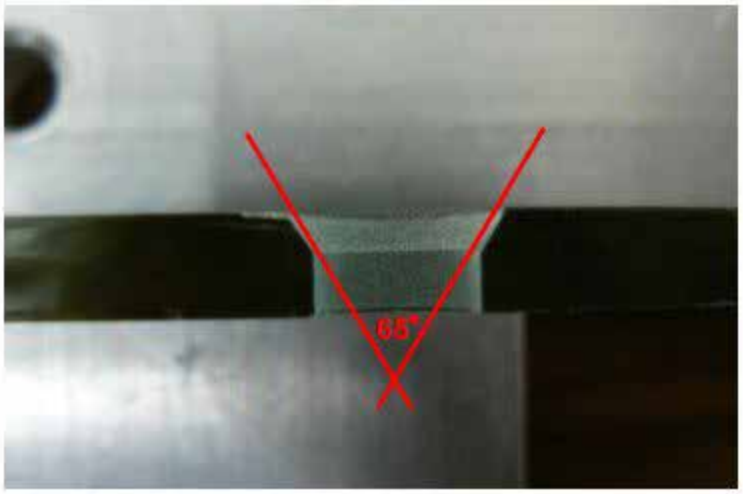

Cutting by Ablation-Applications

Green laser 532nm – DPSS SHG

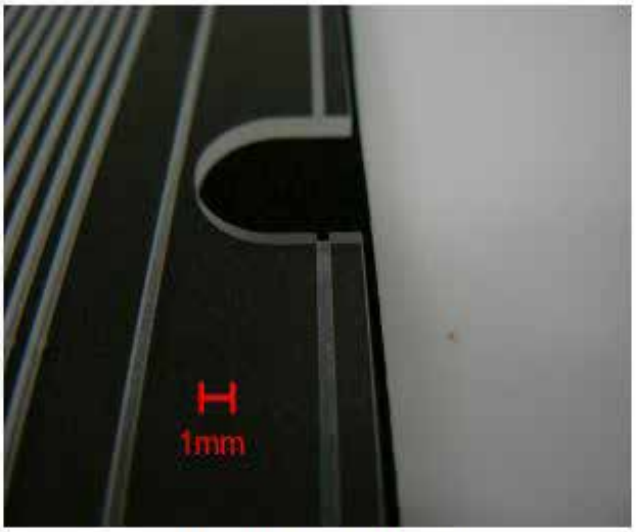

Combination of drilling and marking

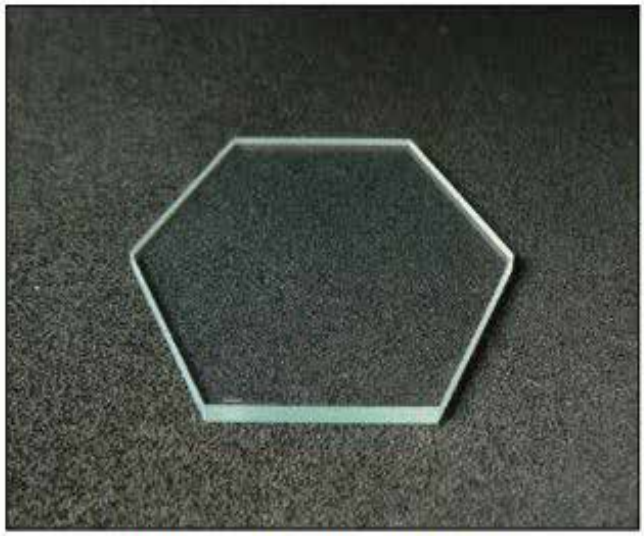

Flexible layouts with high shape accuracy

Green laser 532nm – DPSS SHG

Glass thickness 10mm

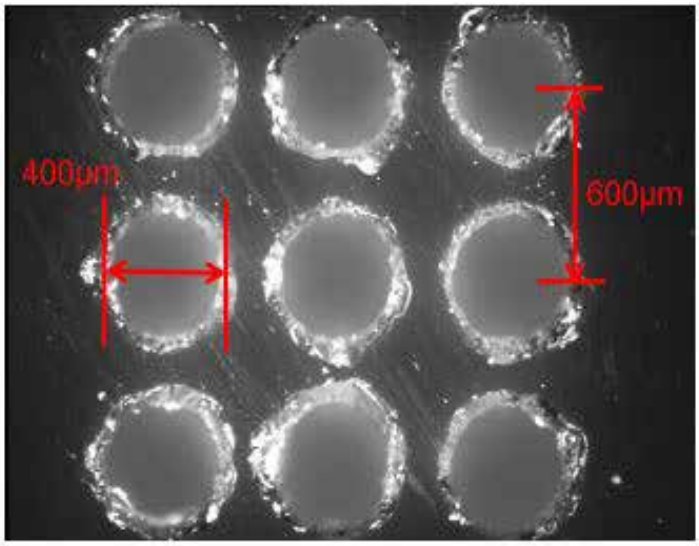

Ø 0.4mm holes in 10mm sodalime glass

Cutting by Ablation-Machine

Laser driller LD Series

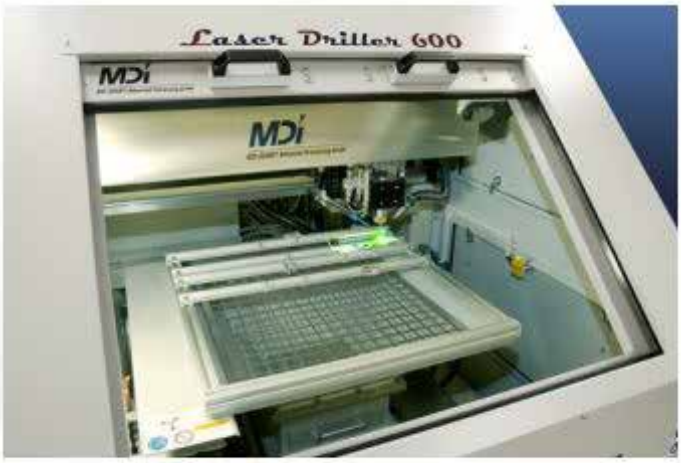

Laser driller LD600

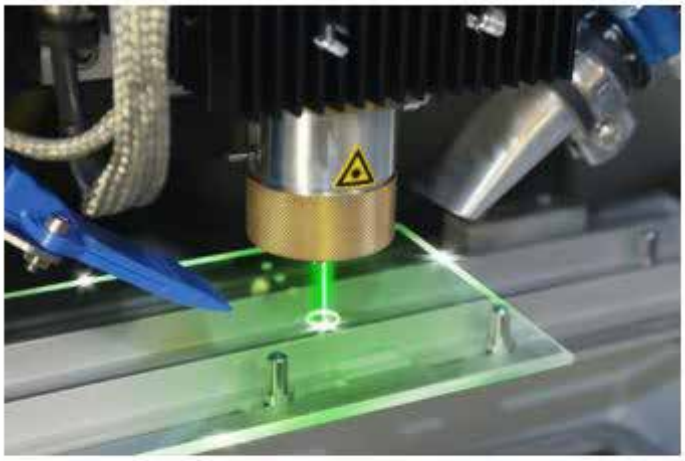

Drilling process

Green laser 532nm – DPSS SHG

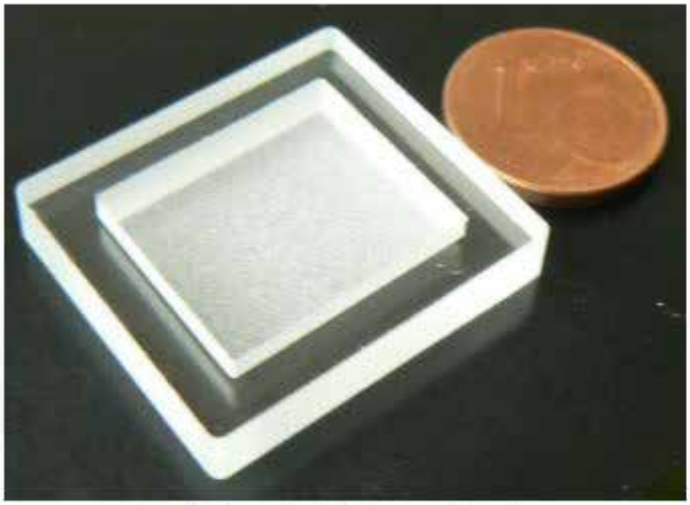

Sagging 2mm depth in 3mm sodalime glass

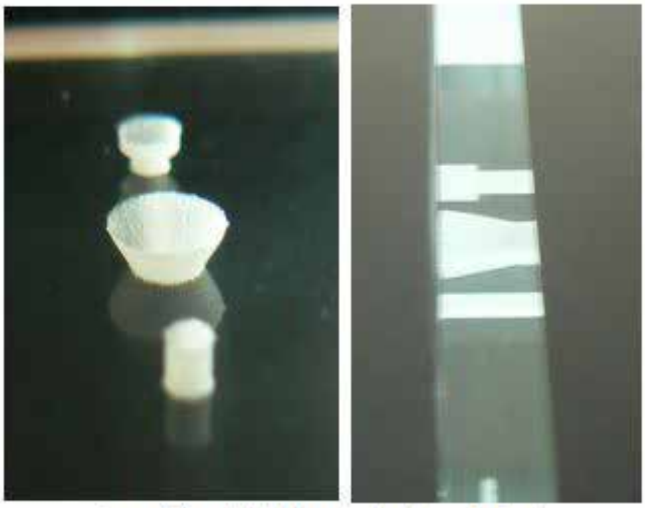

1mm drilling (straight, conical and counterbore)

NANOXSOLAR
A division of IIXS Technologies, Inc.

Filament Cutting

Effect of pulse width on processing with nanosecond lasers

Longer pulses:
much of the pulse energy contributes only to heating Heat can spread into surrounding material and cause damage known as heat-affected zone (HAZ)

Shorter pulses:
higher proportion of pulse energy is delivered above the threshold power level, & maximizing processing while minimizing HAZ

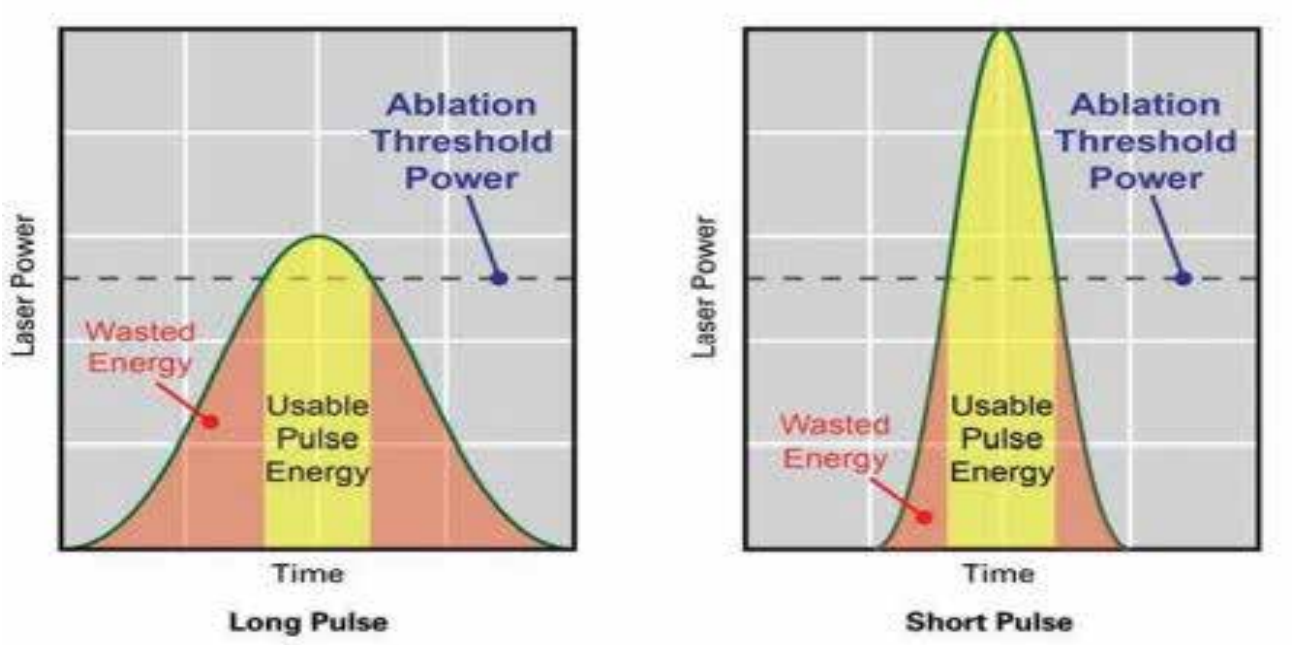

Comparison: laser micro machining vs. filament cutting

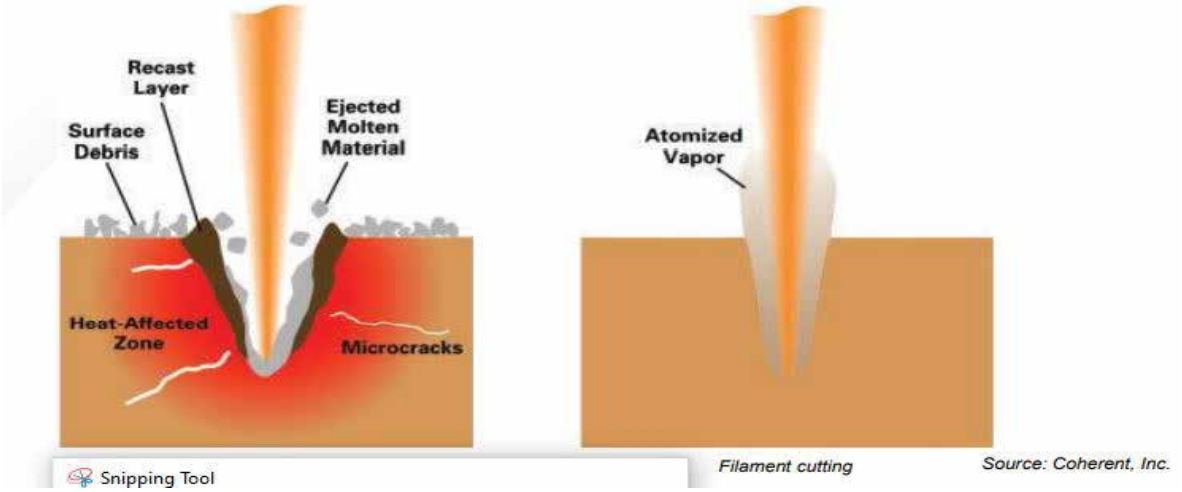

Filament Cutting

Technology:

- ps-laser pulses are focused within transparent material
- High local intensity gives rise to self focusing
- Different from ablative process – no debris
- Hot free-electrons damage / melt material
- Filament creates a defect channel up to 3mm long
- Moving the beam and / or the material creates a curtain of fractures

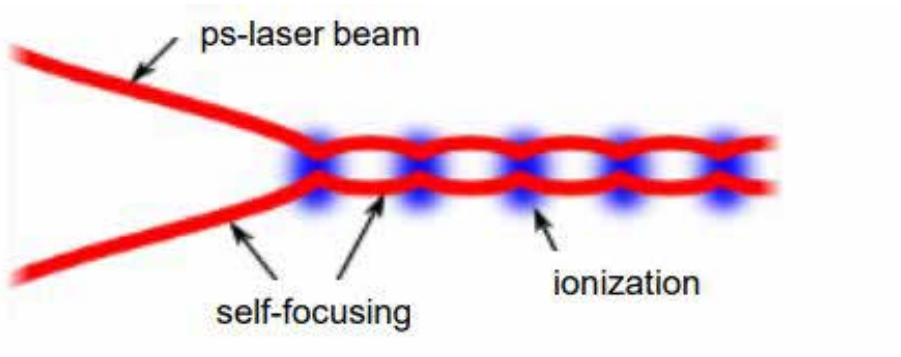

Advantages

- After breaking glass has ground-like surface
- Good bend strength
- Filaments extend through glass
- Minimal micro cracks
- No surface mark or debris
- Curved cuts possible

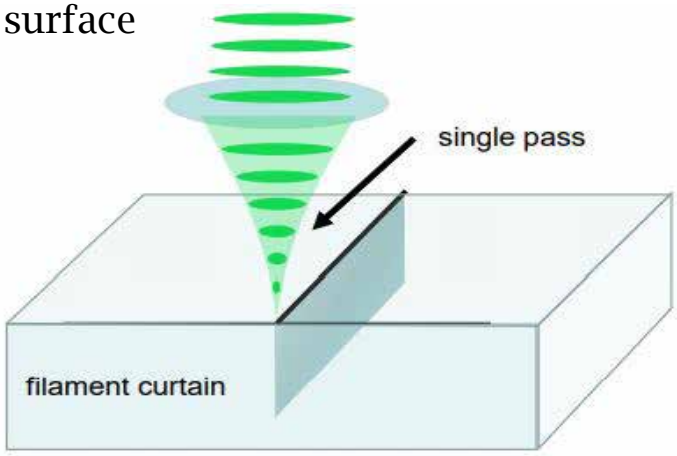

Conclusion

Wheel cutting:

Market introduced and investment is low,
but chips (not clean) and poor edge strength require post processing.

CO2 laser:

Offers high edge strength and is clean,
but limited capability in geometry and rectangular edges are disadvantageous.

UV and green laser (ablation):

Higher invest than wheel machines, advantages in “glass inside“ (holes, any kind of shape).

Filament cutting / ps laser:

Good for strengthened glass, capability for free shapes, medium edge strength. Economical benefit not clear; more R&D is needed.

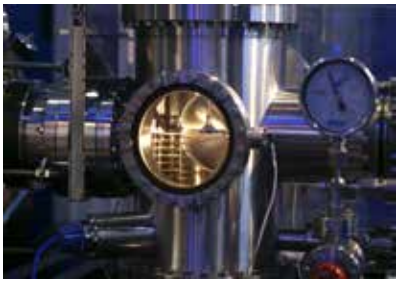

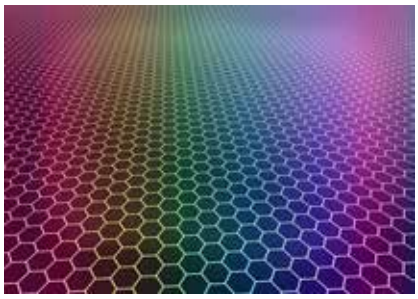

Materials and Design for Architectural Applications

Visible transmission
As high as possible
VLT ~ 75% (typ.)

Heat management for architectural applications
Thermal
Solar control

Reflection
Codes in many major cities
specify <20%

Interactions with Electromagnetic Spectrum

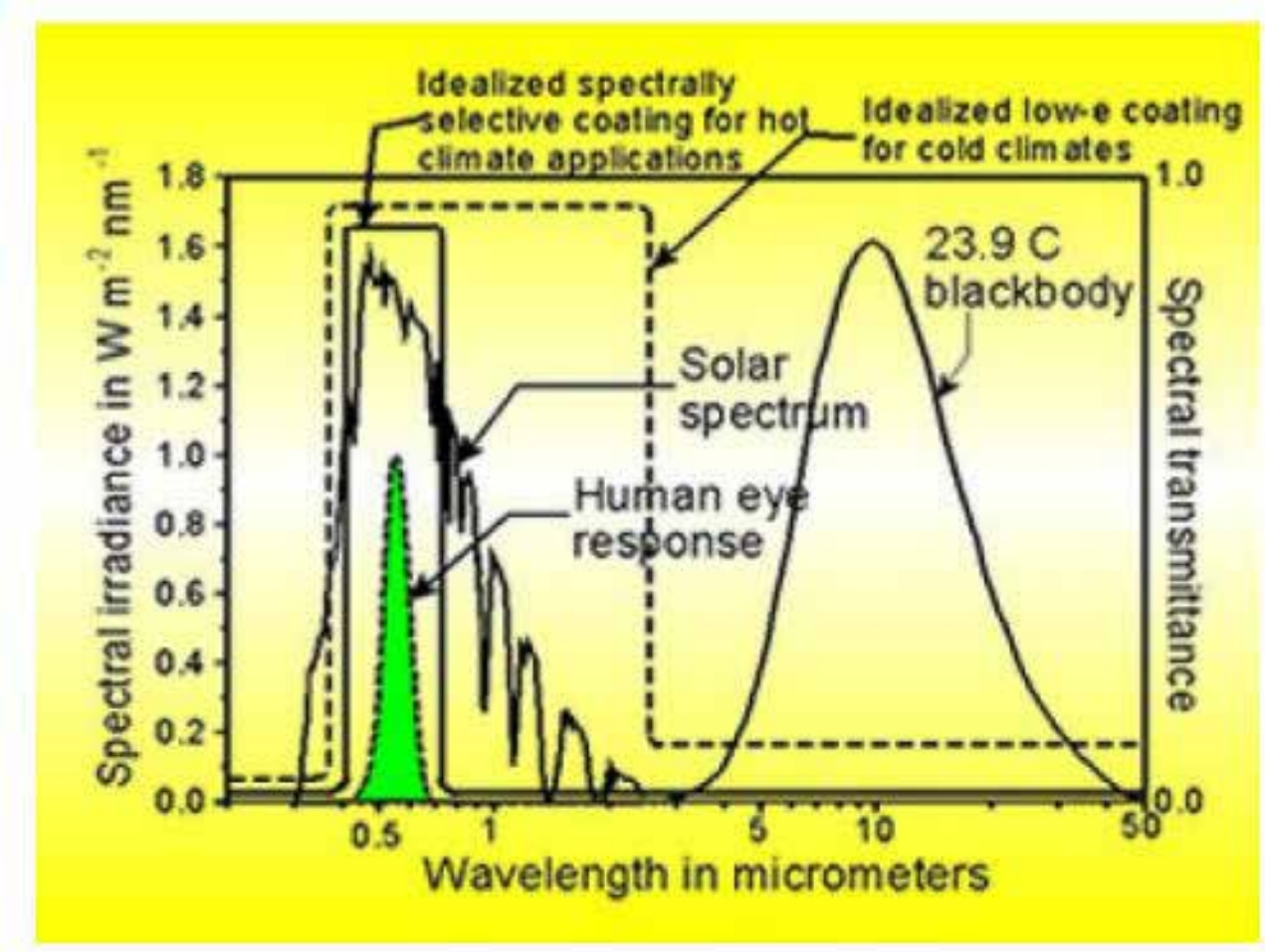

Materials Design – Optical Response

Fluorine doped SnO 2 (FTO, SnO 2:F)

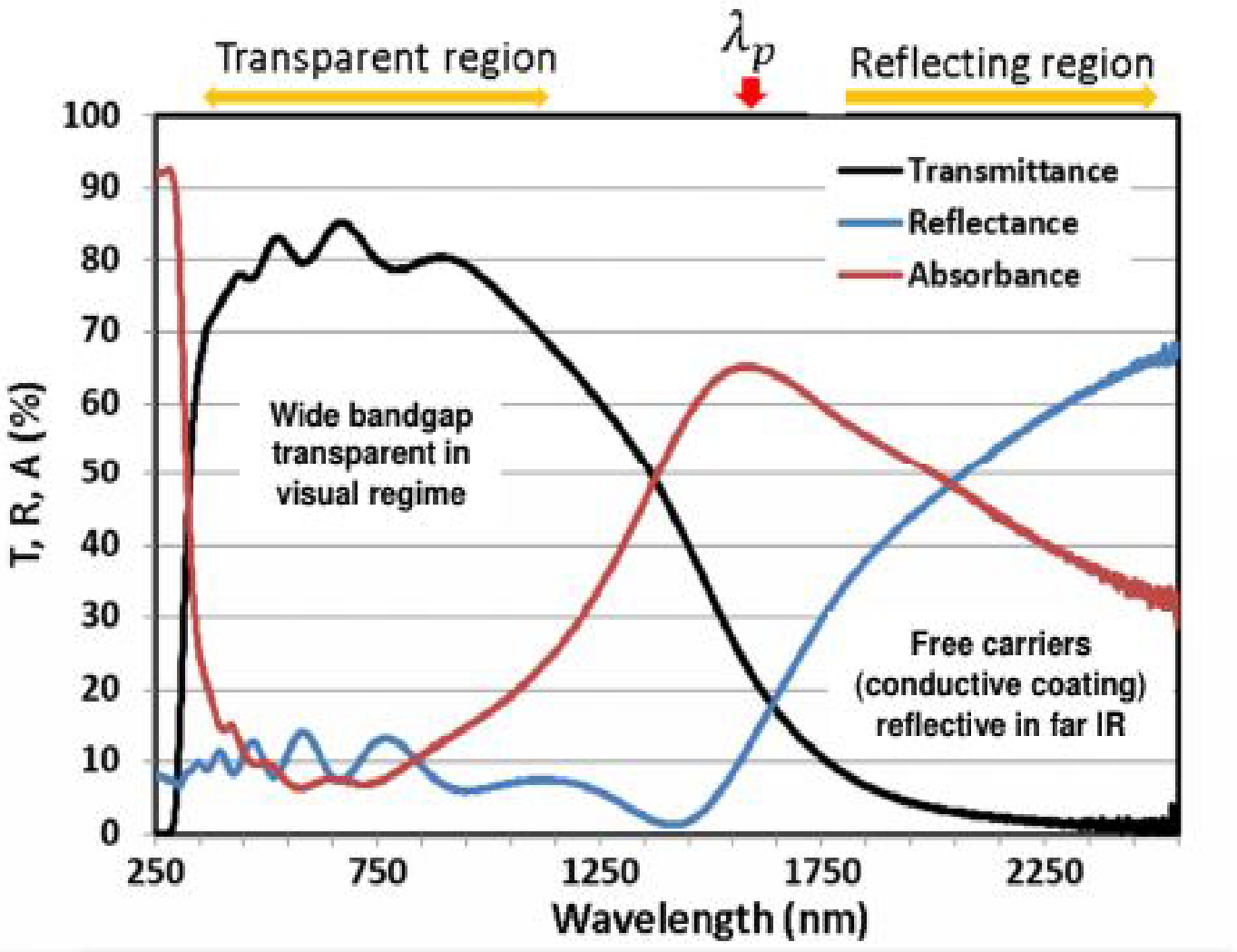

Materials and Design for Architectural Applications

Emissivity For an object exposed to a thermal / blackbody source

$$Absorbed\ Energy = \alpha_\lambda E_{b\lambda}(\lambda, T)$$

$$Emitted\ Energy = \varepsilon_\lambda E_{b\lambda}(\lambda, T)$$

where ε_λ is the emissivity of the object at wavelength λ

At thermal equilibrium

$$Emitted\ Energy = Absorbed\ Energy$$

Leading to $\varepsilon_\lambda = \alpha_\lambda$ (Kirkoff's law)

The average emissivity then is

$$\bar{\varepsilon} = \frac{\int_0^\infty \varepsilon_\lambda E_{b\lambda}(\lambda, T)\, d\lambda}{\int_0^\infty E_{b\lambda}(\lambda, T)\, d\lambda}$$

Or (invoking Kirkoff's law)

$$\bar{\varepsilon} = \frac{\int_0^\infty \alpha_\lambda E_{b\lambda}(\lambda, T)\, d\lambda}{\int_0^\infty E_{b\lambda}(\lambda, T)\, d\lambda}$$

Where α_λ is (reasonably) measurable in the lab

NANOXSOLAR
A division of NXS Technologies, Inc.

Materials and Design for Architectural Applications

Emissivity of Uncoated Glass

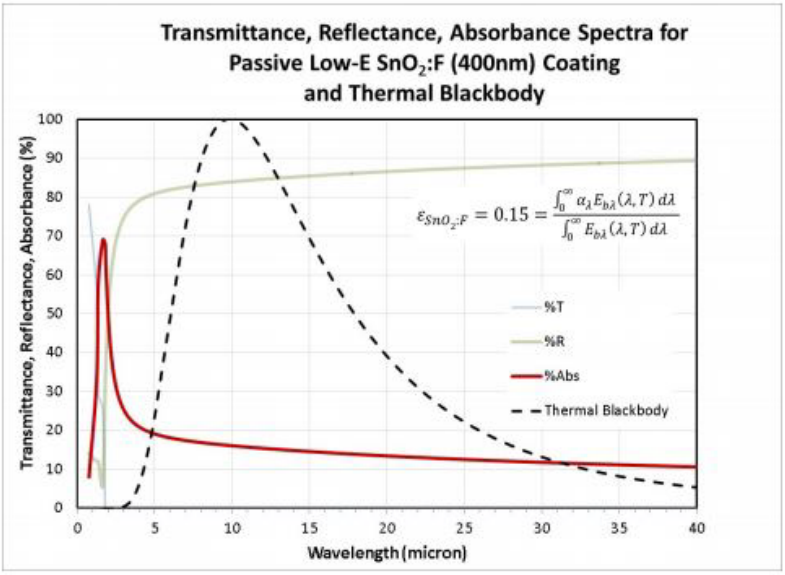

Emissivity of SnO2:F Conductive Coating

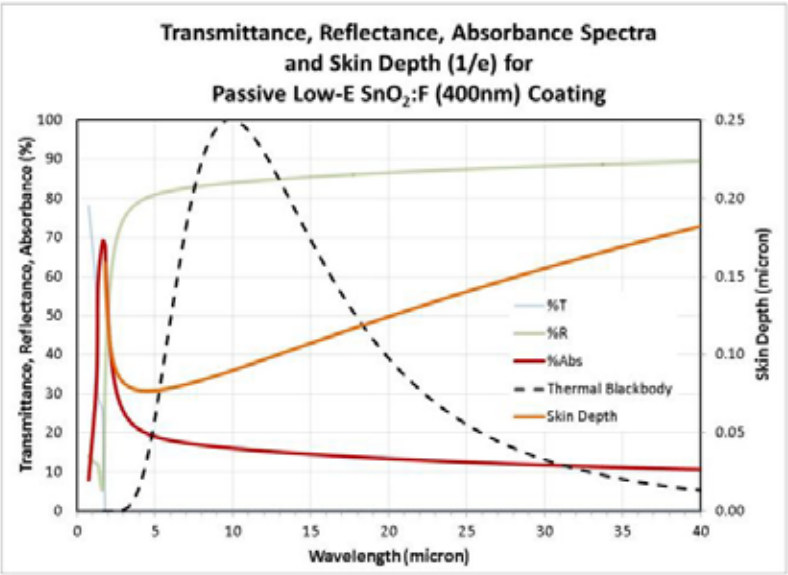

http://www.nanoxsolar.com/

NANOXSOLAR
A division of IXS Technologies, Inc.

Materials and Design for Architectural Applications

Skin Depth (1/e) of Conductive SnO2:F Coating

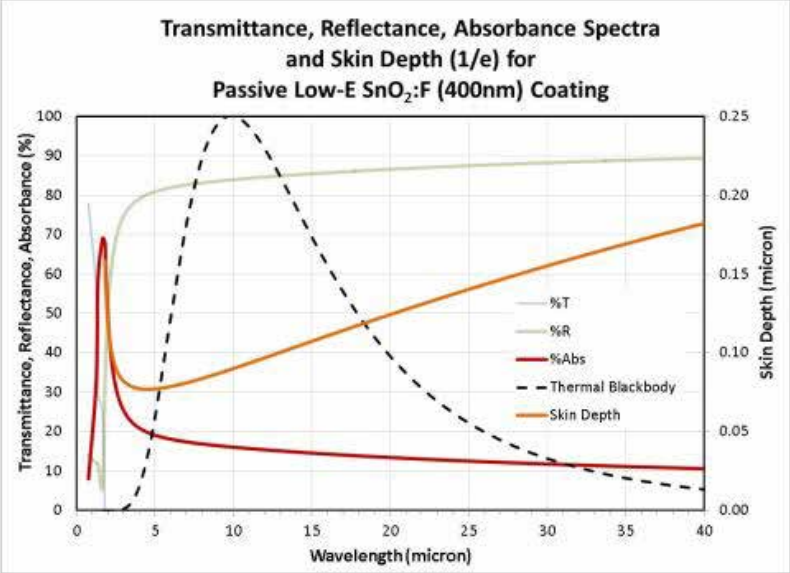

Emissivity control

Coating thickness
Doping efficiency

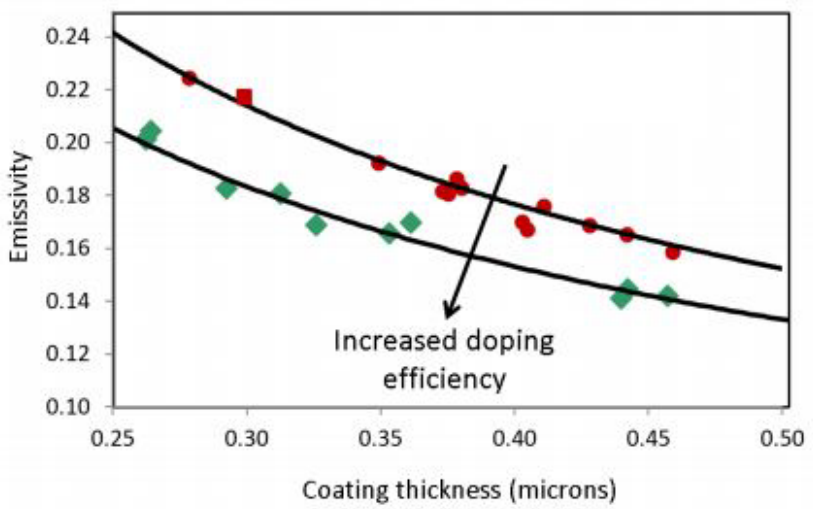

NANOXSOLAR
A division of IMX5 Technologies, Inc.

Materials and Design for Architectural Applications

Growth modes

Amorphous layers

Flat interfaces

Crystalline/columnar growth

Crystal quality improves with increased thickness

Increased surface roughness

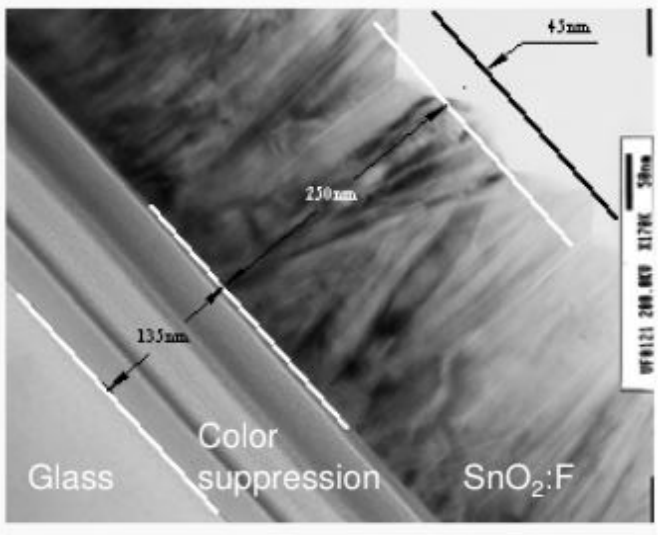

Heat transfer mechanisms

Radiation transport– thermal regime

Parallel surfaces

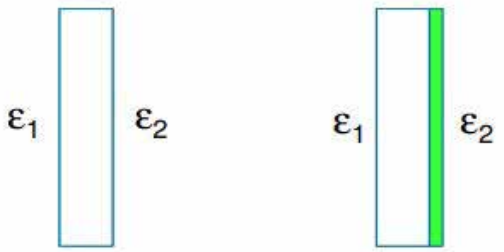

$$Q_{rad} = \frac{4\sigma T^3}{(\frac{1}{\varepsilon_1} + \frac{1}{\varepsilon_2} - 1)}$$

$\varepsilon_{glass} = 0.84$

$\varepsilon_{CVD} = 0.23$

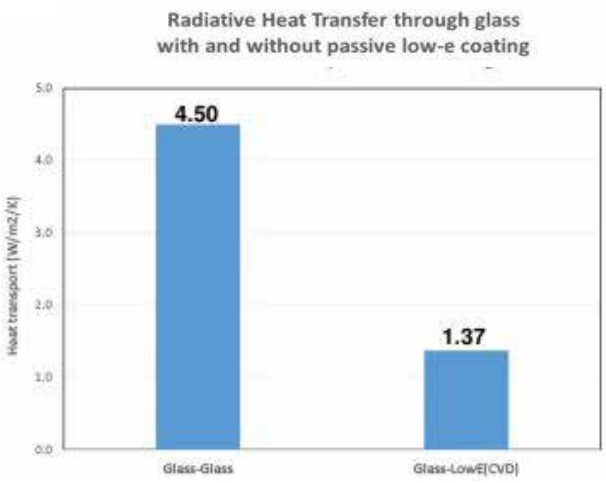

Materials and Design for Architectural Applications

Windows design for reduced heat transfer

Heat transfer mechanisms
- Convection
- Conduction

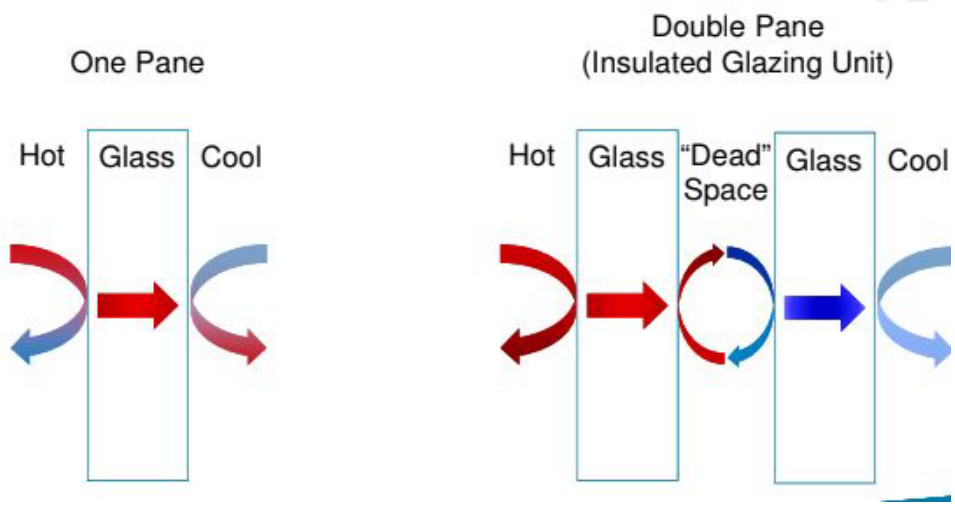

Window Design

$$Heat\ transfer = U * A * \Delta T$$

Single pane clear glass U = 1.11

Type: Pyrolitic Low-E Clear Insulating Glass
"Sungate®" 500 (2) Clear + Clear **by PPG Industries, Inc.**

Outdoor Lite: Clear Glass, Pyrolytic Coated on second surface (2)
Indoor Lite: Clear Float Glass
Low-E Coating: ***"Sungate"*** 500 (Pyrolitic) by PPG Industries, Inc.
Location: Second Surface (2)

Performance Values

Visible Light Transmission	U-Value Winter	U-Value Summer
74%	0.35	0.35

Insulating Glass Unit (IGU) window with CVD low-e coating reduces energy loss by 3X as compared with windows with single pane of glass

NANOXSOLAR
A division of IXS Technologies, Inc.

Materials and Design for Architectural Applications

Window Design Resources

http://www.nanoxsolar.com/

Materials and Design for Architectural Applications

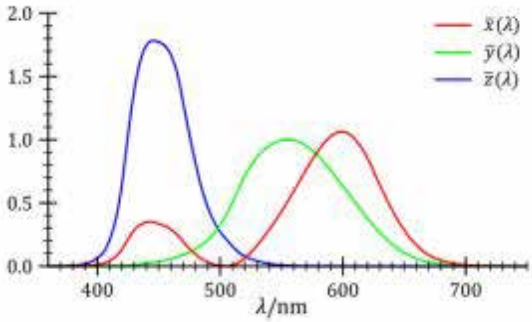

Color can be represented in L*a*b* space

Weighting functions in visual spectrum give
L* - brightness
a* - red/green axis
b* - yellow/blue axis

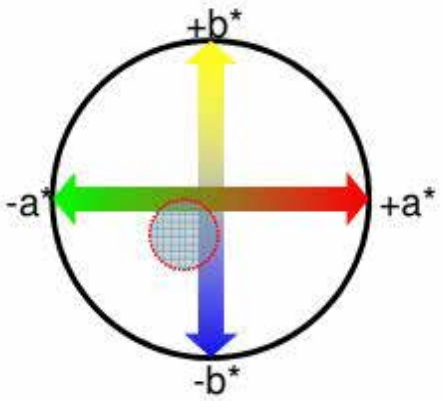

Customers want

Neutral ~ (0,0)
Blue-green (-a*, -b*)

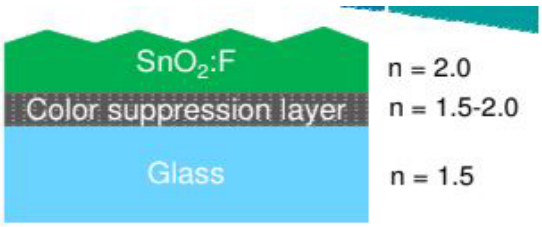

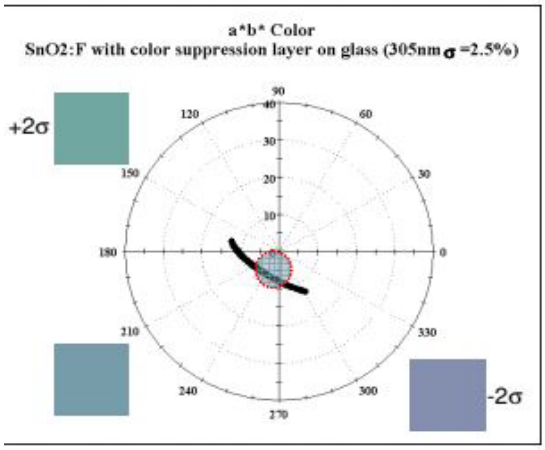

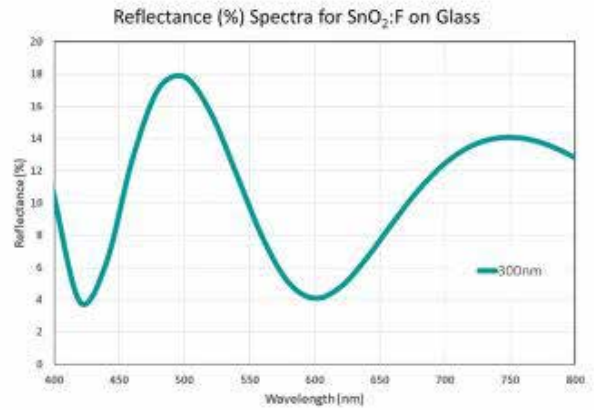

Optical response

Design of coating stack
Response often non-linear in color space

Materials and Design for Architectural Applications

Optical response

Add color suppression layer between high index (SnO2:F) and low index (glass)

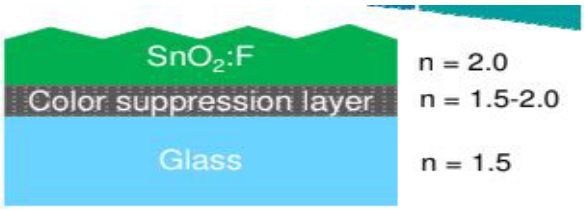

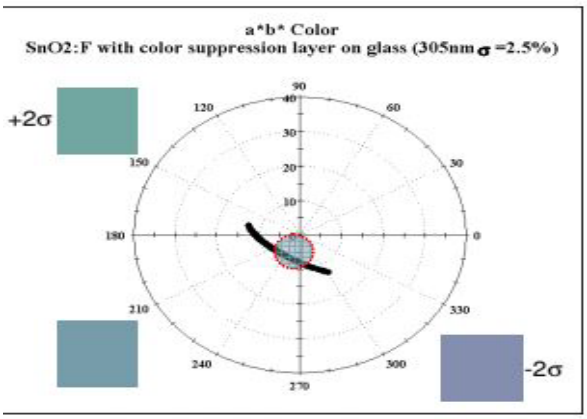

Color suppression layer approaches

Discrete H-L index layers

SnO_2 / SiO_2 / SnO_2 / SiO_2

Homogenous intermediate index layer

$Si_xSn_{(1-x)}O_{(2-\delta)}C_\delta$

Graded optical index

Mixed metal oxides

$Si_xSn_{(1-x)}O_2$ (x is a function of layer thickness)

$Si_xTi_{(1-x)}O_2$ (x is a function of layer thickness)

Chemistry for CVD Coatings Typical precursors

SnO2

- Monobutyl tin trichloride ($C_4H_9SnCl_3$)
- Bibutyl tin dichloride ($(CH_3CH_2CH_2CH)_2SnCl_2$)
- Trimethyl tin ($C_4H_{12}Sn$)

F

- Hydrofluoric acid (HF)
- Trifluoroacetic acid ($C_2HF_3O_2$)

SiO2

- Tetraethyl orthosilicate ($SiC_8H_{20}O_4$ - TEOS)
- Silane (SiH_4)
- Monochlorosilane ($SiClH_3$)

TiO2

- Titanium isopropoxide ($C_{12}H_{28}O_4Ti$)
- Titanium tetrachloride ($TiCl_4$)

NANOXSOLAR
A division of IXS Technologies, Inc.

Materials and Design for Architectural Applications

Choosing a precursor – criteria to consider

Safety

Toxic (acute, chronic exposure)
Flammable / pyrophoric
Asphyxiate (CO_2 vs N_2 vs NF_3)

Compatibility with other precursors

$2MCl_3 + 3H_2O$----> $6HCl + MO_x + yO_2$ (~instantaneous, exothermic)

Deposition efficiency within desired / allowable temperature regime

Cost

http://www.nanoxsolar.com/

Process and Equipment

Process & Equipment – basic unit operations

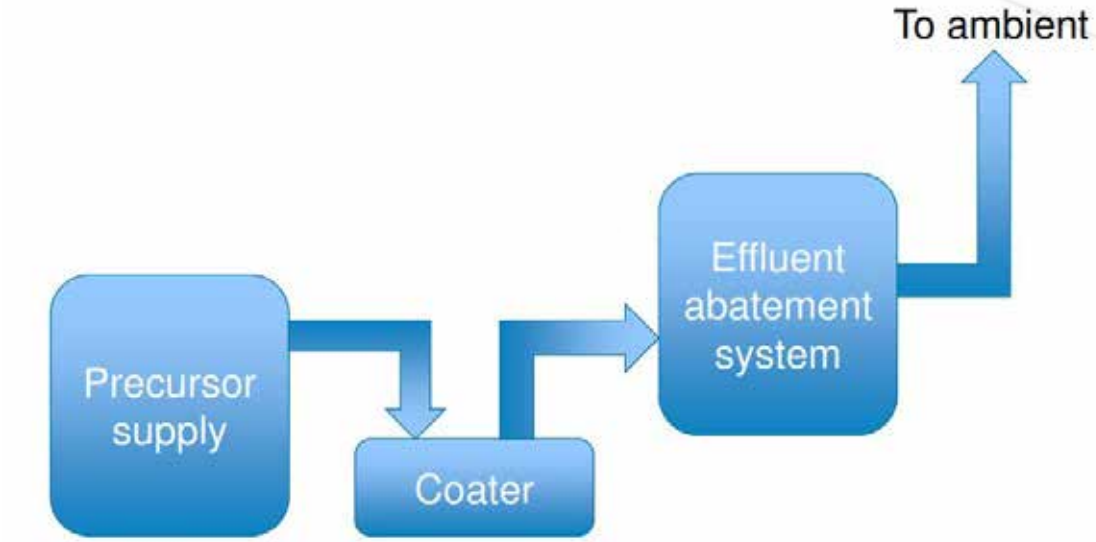

Process & Equipment – coater location

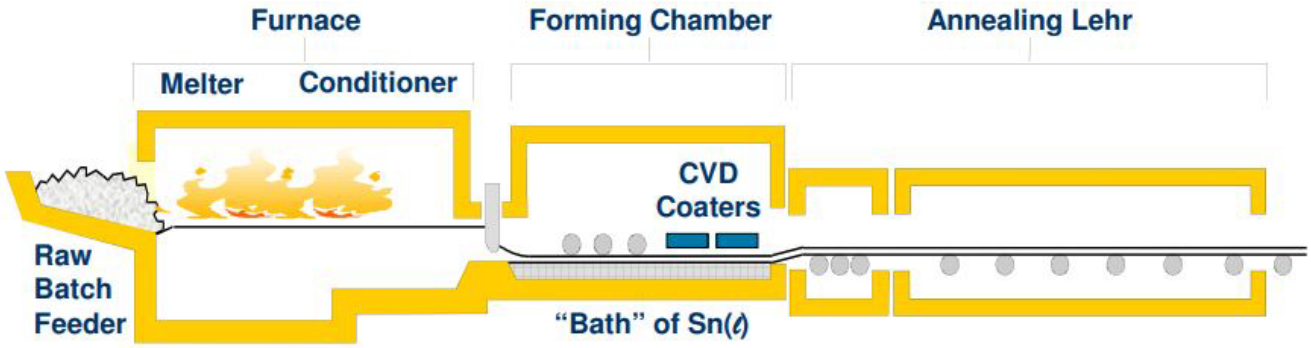

Float glass
– 25 MM m2/yr per line

Online CVD coating
– 10 MM m2/yr per line

Efficient use of energy
Use existing energy content of the glass

Glass Temperature = 600-675˚C
Glass Speed = 5 to 15 meters/min.

Process and Equipment

Precursor flow system

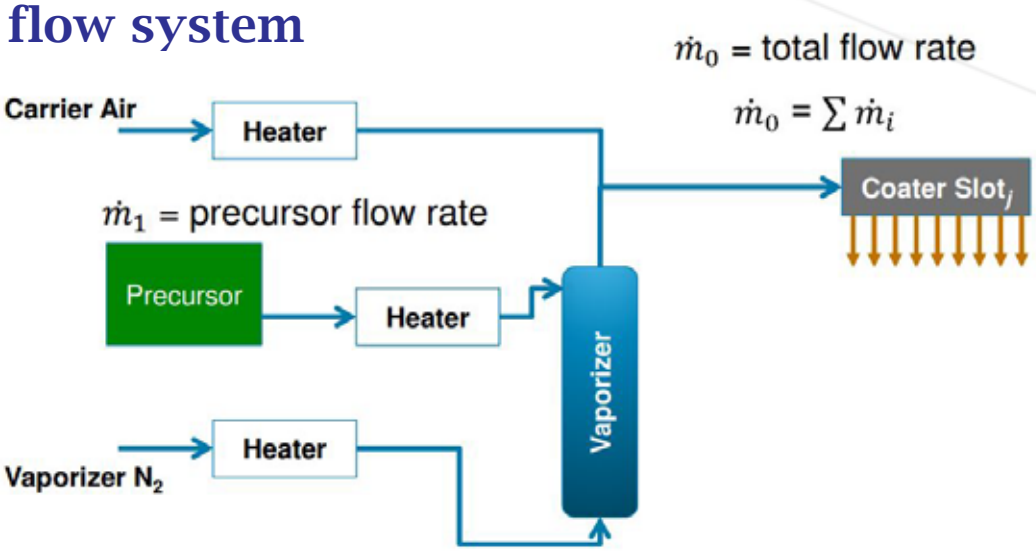

Process & Equipment – precursor vaporization

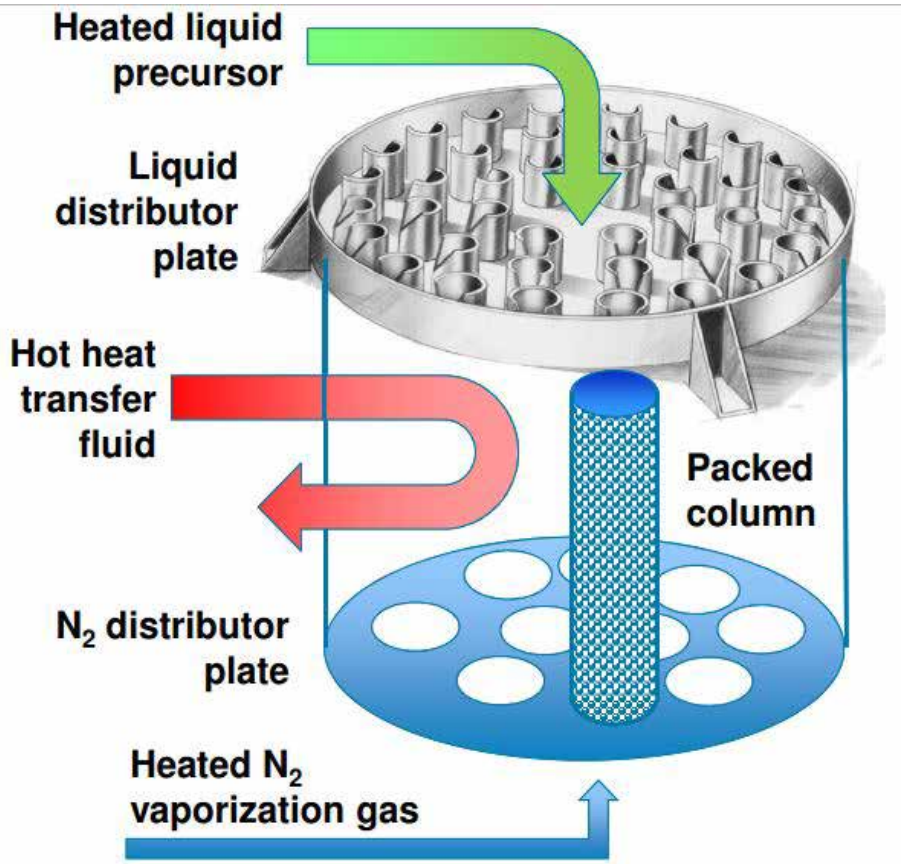

Liquid distributor fouling resistance (best to worst)
- V-notch weir
- Spray
- Slotted weir
- Sidewall orifice

Packing types
- Metal chips
- Raschig rings
- Pall rings

Process and Equipment

Process & Equipment – vaporizer operations

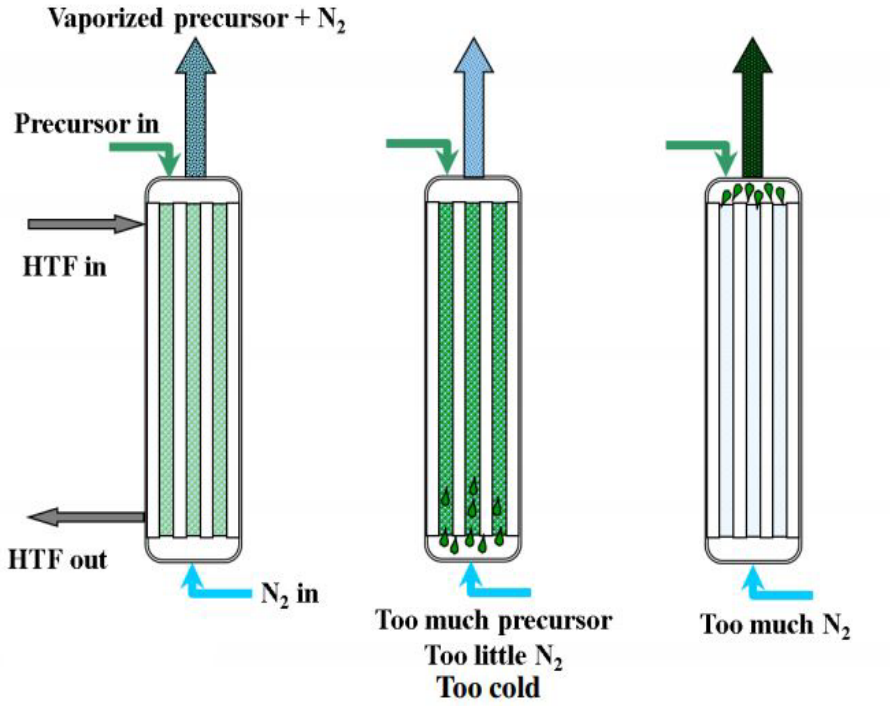

3 potential operating conditions

Process & Equipment – vaporizer operation

What is the operating temperature for vaporization of MBTC
- 36.5 lb/hr MBTC flow
- 20 SCFM N_2

MW_{MBTC} = 282 lb / lb-mol
N_2 std vol = 386.7 SCF / lb-mol
MBTC concentration = 4%

T_{op} > 271 F
Condensation temperature (F) of MBTC as a function of vapor phase concentration
- If T_{op} < 270F expect liquid into pot

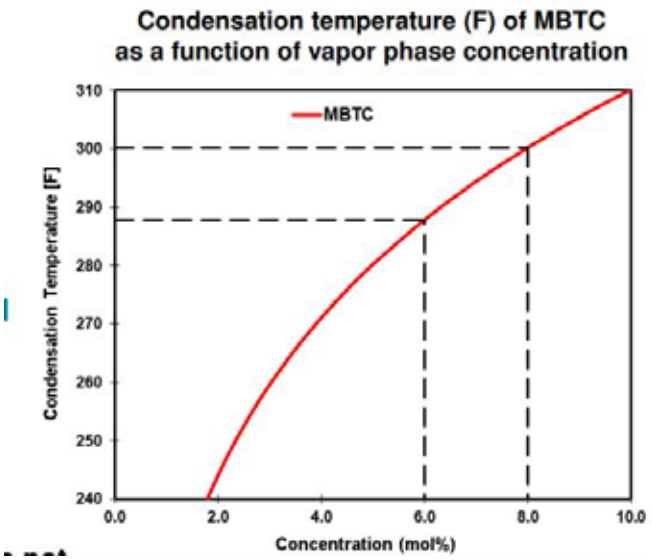

Process and Equipment

Process & Equipment – vaporizer operation

Souder-Brown equation predicts entrainment when velocity V in the vaporizer packed column is greater than V_G

54.75 lb/hr MBTC 30 SCFM N_2 T=300 F

ρ_{MBTC} = 91.95 lb/ft^3 ρ_{vap} = 0.0531 lb/ft^3

12 tubes (1-1/4" sch 10) ID = 1.442"

$V_{vap+chem}$ = 5.49 ft/s V_G = 4.93 ft/s

Souder-Brown Eqn.

$$V_G = k\sqrt{\frac{\rho_L - \rho_G}{\rho_G}}$$

For packed column
k = 0.175 ft/s

Entrainment is expected "coater drip"

Process & Equipment – basic coater design

Single inlet and exhaust

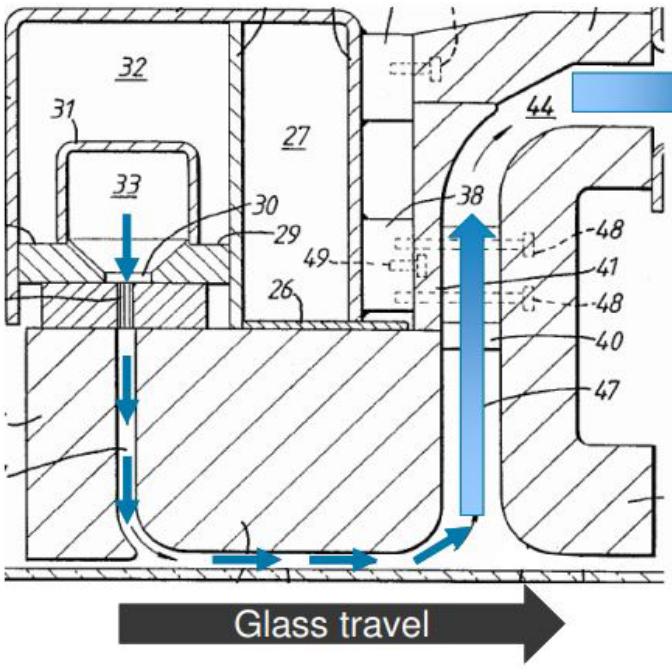

US Patent 4,857,097
R.F Berry, 1989

Process and Equipment

Process & Equipment – basic coater design

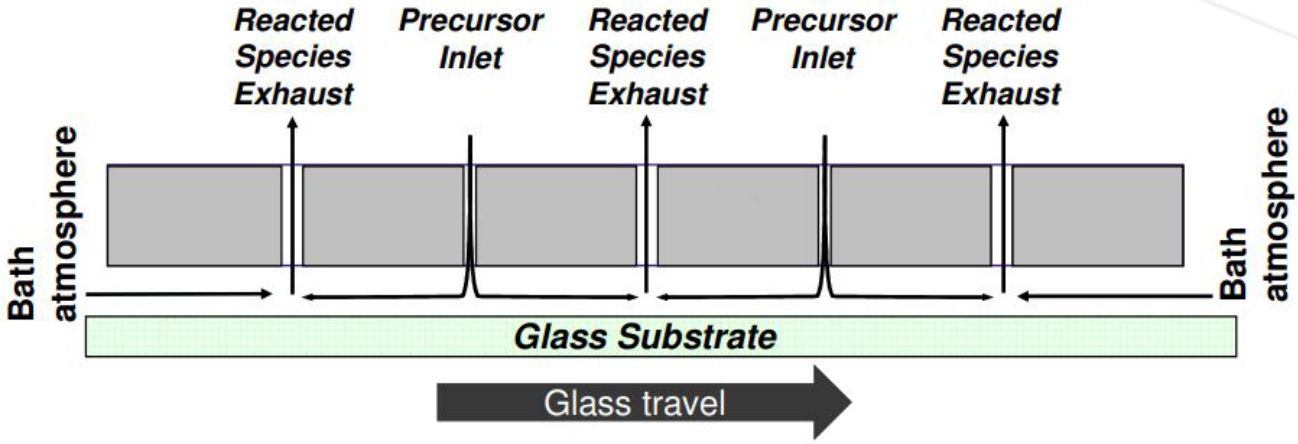

Flows and temperatures under coater

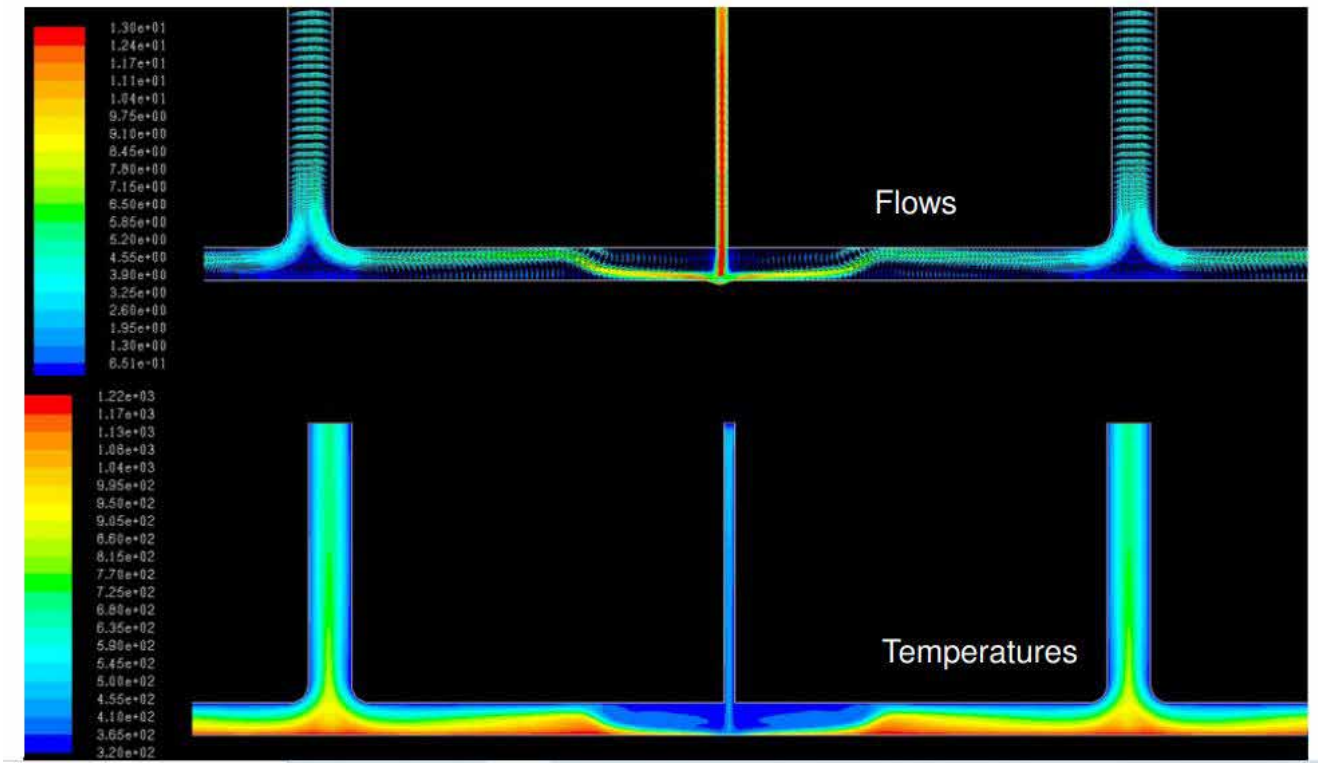

Process and Equipment

Deposition mechanism

2 mechanisms: (1) mass transport, (2) reaction at surface

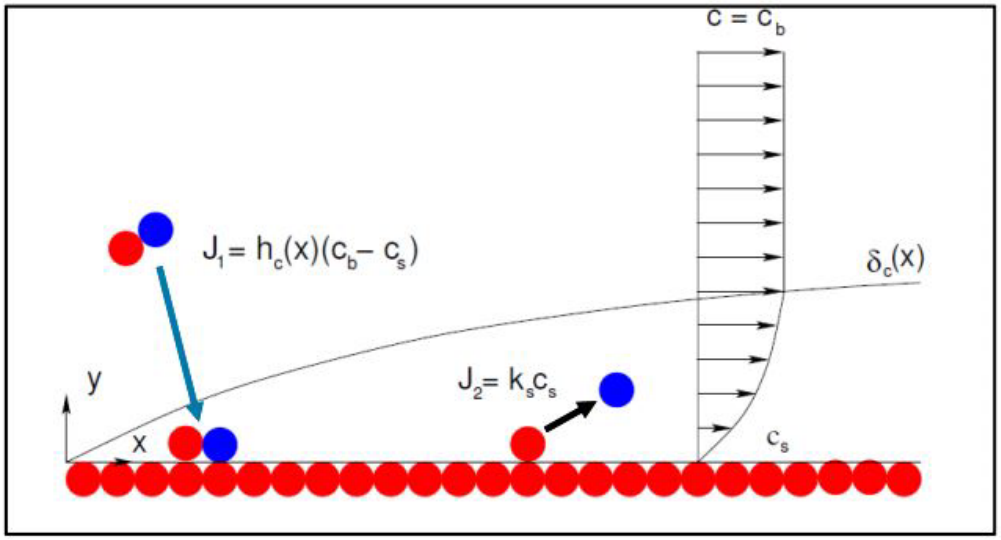

$$J = \frac{c_g}{\delta/D + 1/k_s}$$

$$J = \frac{c_g}{\delta/D} \qquad J = C_g k_s = C_g e^{-E/kT}$$

$$\delta(x) \propto \sqrt{x/u} \qquad T = F(x)$$

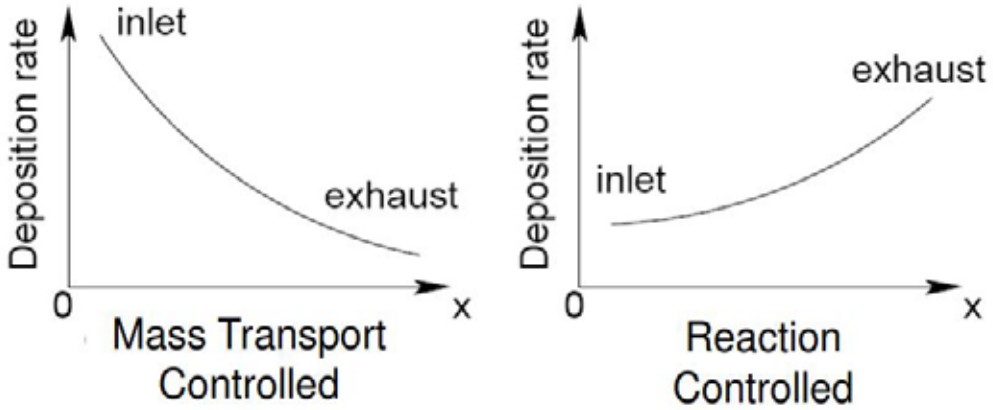

Process and Equipment

SnO2 deposition from MBTC

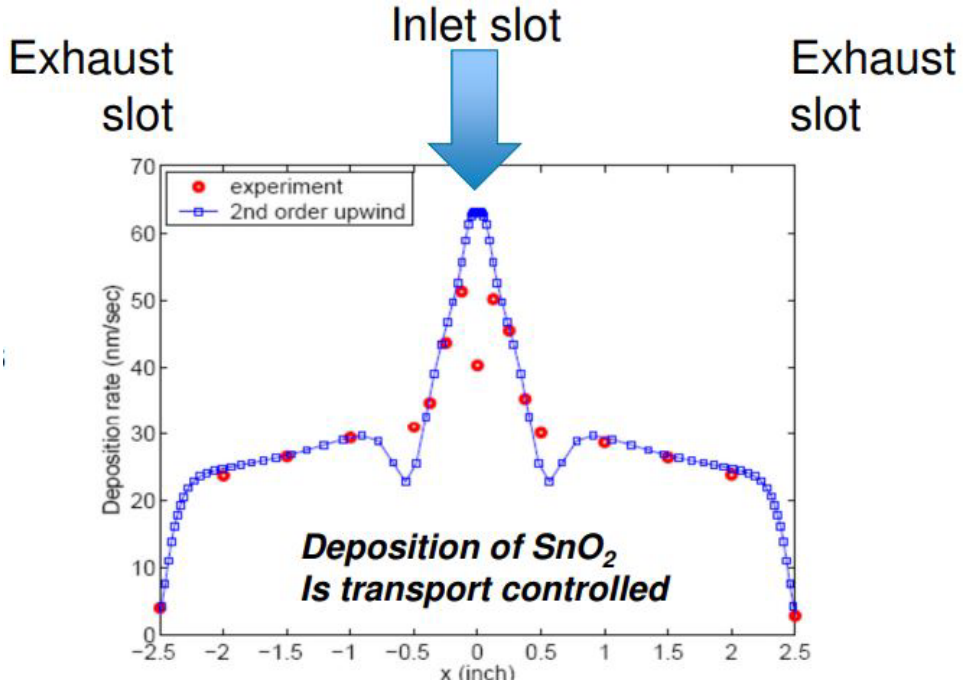

Stationary glass experiment

Addition of H2O to precursor stream

Stagnate flow reactor experiments (PPG & LBNL studies)

Change from reaction control to transport control for T > 375C

Addition of H2O accelerates the reaction

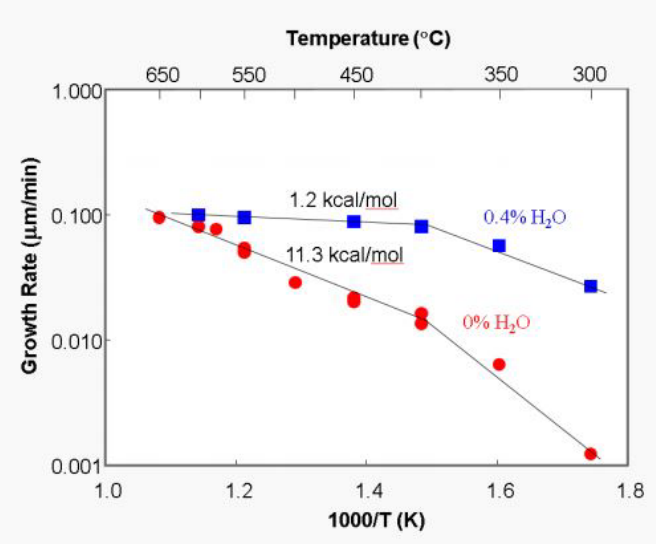

Process and Equipment

Deposition mechanism – mass transport

For N slots with
- L = the length between inlet and exhaust
- u = velocity of vapor
- x = distance from inlet
- ν = velocity of glass
- C_g = concentration of chemistry far from the surface

We can write for the coating thickness[h]

$$h \propto \frac{N\int_0^L \left(c_g\sqrt{\frac{u}{x}}\right)dx}{v} \propto \frac{N\cdot c_g\cdot u^{1/2}\cdot L^{1/2}}{v}$$

But

$$u \propto \frac{\dot{m}_0}{N\cdot H}$$

$$c_g \propto \frac{\dot{m}_1}{\dot{m}_0}$$

Where
m_0=total mass flow rate (precursor + carrier gas)
m_1=precursor flow rate
H= coater height above the glass

Such that… $$h \propto \sqrt{N\cdot L}\cdot\frac{\dot{m}_1}{\sqrt{\dot{m}_0}}\cdot\frac{1}{\sqrt{H}}\cdot\frac{1}{v}$$

$$J = C_g e^{-E/kT}$$

Similar to the mass transport case

$$h \propto \frac{\dot{m}_1}{\dot{m}_0}\frac{e^{-E/kT}}{T}\frac{L}{v}$$

Process and Equipment

Materials and Design

Low maintenance coatings ("self cleaning")
TiO_2
Low surface energy when clean– hydrophilic

Wide bandgap semiconductor– produces e-h pairs with UV

Design of Experiments – ask what controls thickness

$$\frac{\dot{m}_1}{\sqrt{\dot{m}_0}} \cdot \frac{1}{\sqrt{H}} \frac{\sqrt{T}}{v} \qquad \frac{\dot{m}_1}{\dot{m}_0} \frac{e^{-E/kT}}{T} \frac{1}{v}$$

Thickness	$\dot{m}_0$	H	T
h_1	$\dot{m}_0(1)$	H(1)	T(1)
h_2	$\dot{m}_0(2)$, $\dot{m}_0(2')$	H(2)	T(2)
h_3	$\dot{m}_0(3)$	H(3)	T(3)

NANOXSOLAR
A division of IXS Technologies, Inc.

Process and Equipment

TiO2 deposition from titanium isopropoxide

Online experiments
1)Deposition is mass transport controlled
2)Knowledge of mechanism guides process efficiency improvements

$$\eta = \mathcal{F}(\dot{m}_0, \dot{m}_1, \dot{m}_2, H)$$

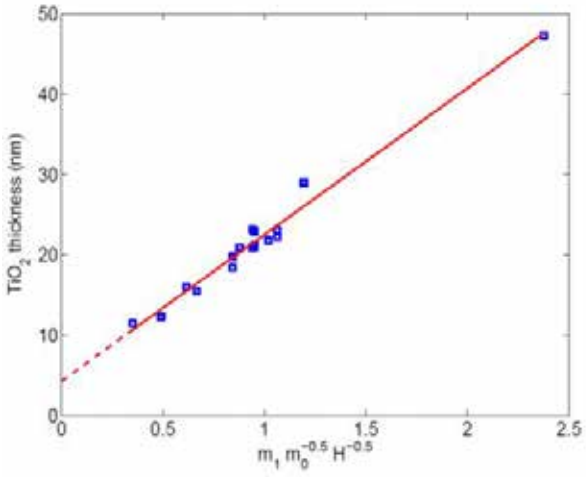

Materials and Design for Solar Applications

Challenges for Solar Applications (Drivers for Technology Development)

Focus on $/$W_p$ and Levelized Cost of Electricity
Energy efficient manufacturing
Device performance
    Optimize for device and application
Durable
    Long term optical performance
    Mechanically durable

Glass and Coated Glass for Thin Film PV
Maximizing Performance is a Multi-factor Optimization

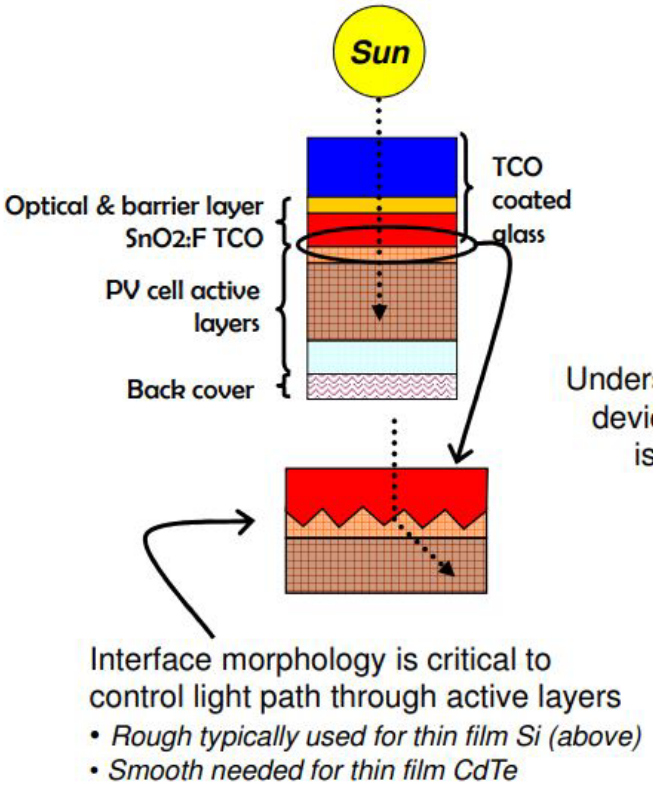

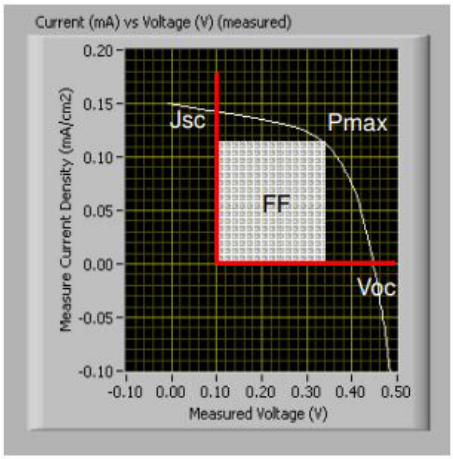

J_{sc}: Light management design

V_{oc}: TCO materials / interface

FF: TCO morphology

NANOXSOLAR
A division of IIX5 Technologies, Inc.

Materials and Design for Solar Applications

Design of High Performance Superstrates TCO Coating Designs

In general electrical and optical properties of the TCO cannot be specified separately

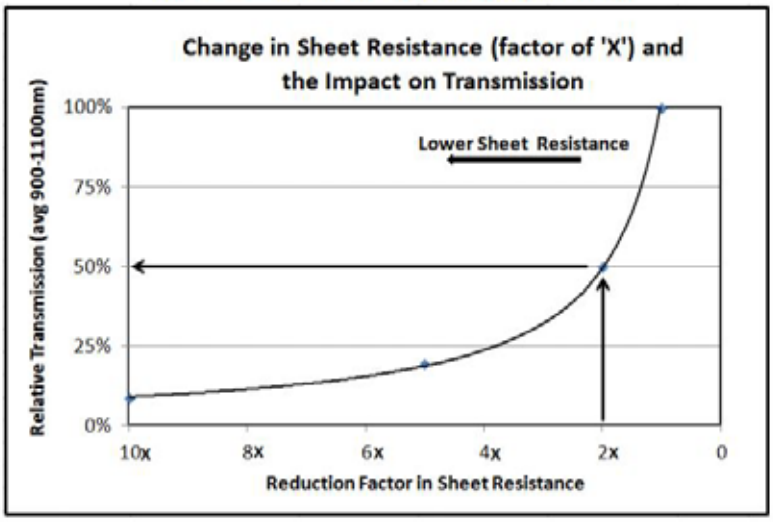

Impact of conductivity on PV performance

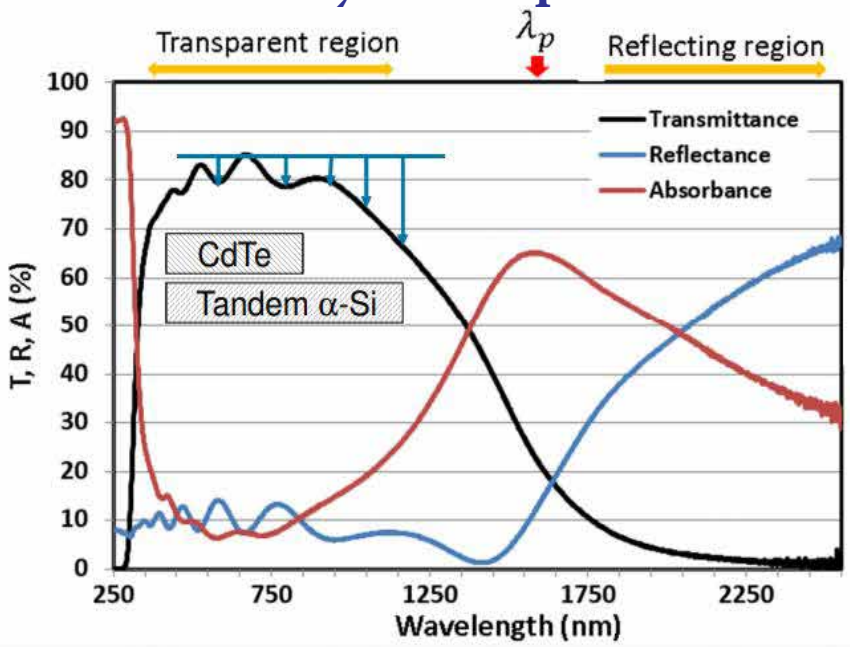

$$\omega_p = 2\pi c/\lambda_p = \sqrt{\frac{ne^2}{\varepsilon_0 \varepsilon_\infty m_e^*}}$$

NANOXSOLAR
A division of IMS Technologies, Inc.

Materials and Design for Solar Applications

Engineering of the Bulk TCO to Reduce Optical Losses

Root causes of losses

1. Intrinsic absorption
2. Free carriers

$$\lambda_p = \frac{2\pi c}{\omega_p} = 2\pi c\sqrt{\frac{\varepsilon_0 \varepsilon_\infty m^*}{ne^2}}$$

3. Bandgap

Materials engineering and design

Film quality
Increase Permittivity
Increase Mobility
Increase Bandgap

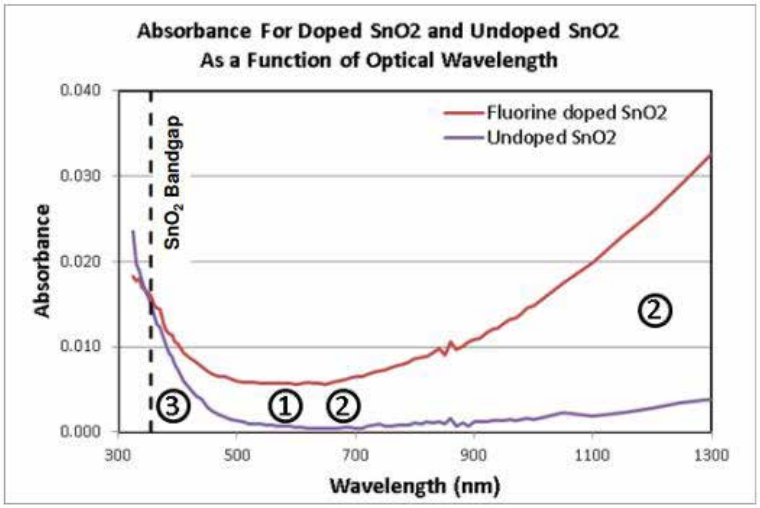

Materials Engineering – reducing optical losses

Alloying of SnO_2 matrix to modify permittivity
Electrical properties comparable to SnO_2:F
Optical properties
comparable to undoped material

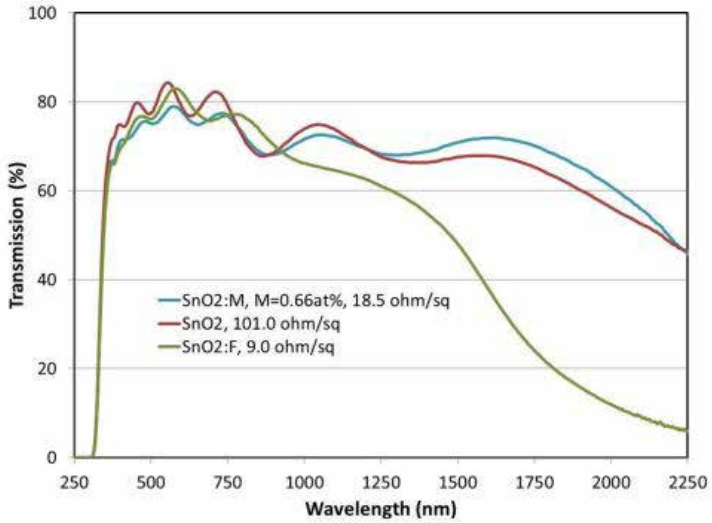

Materials and Design for Solar Applications

Light Redirection by Morphology Engineering

Increased optical path length through PV active layer

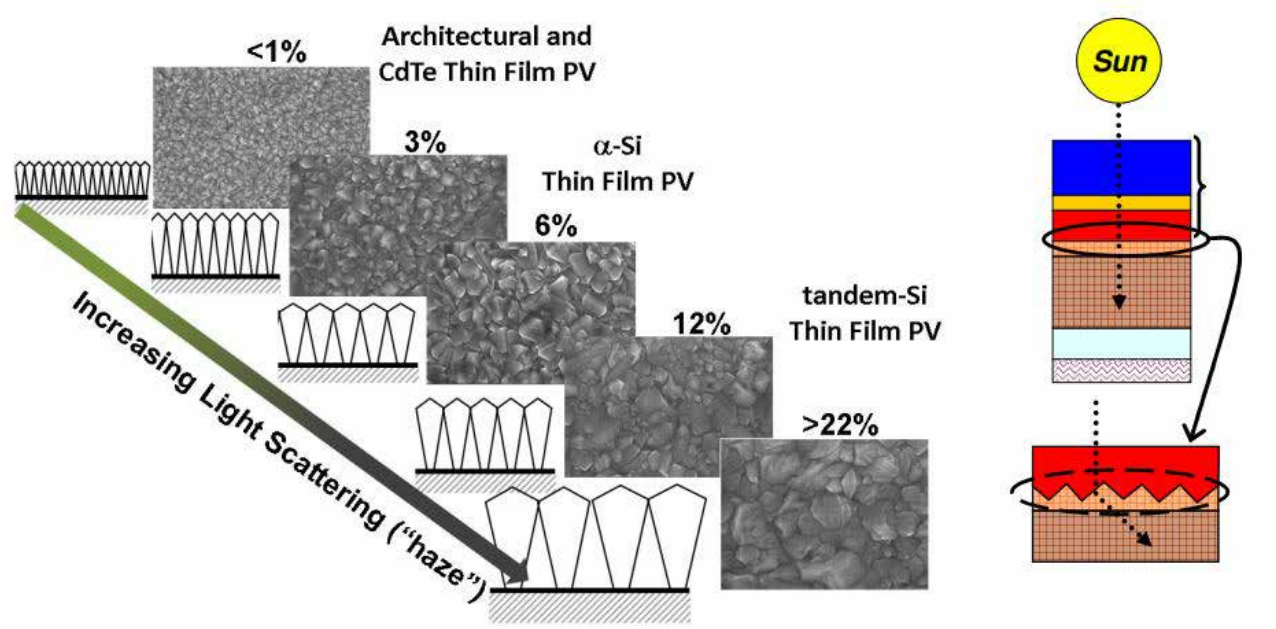

Morphology Design – Tandem α-Si PV

What is optimal crystal size for maximizing scattering in region of interest?

- Small sized-Mie scattering
- SnO-2/Si interface

Optical indices

- Ensemble of sizes form of distribution statistics

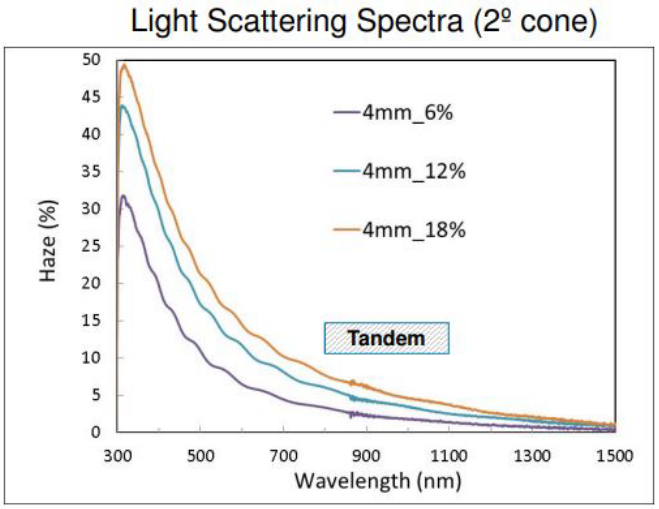

Materials and Design for Solar Applications

Morphology Design Determination of form of Distribution

- Consider an ensemble of grains with distribution ***G***
- Determination of form is difficult in ***R*** space – map into Fourier space

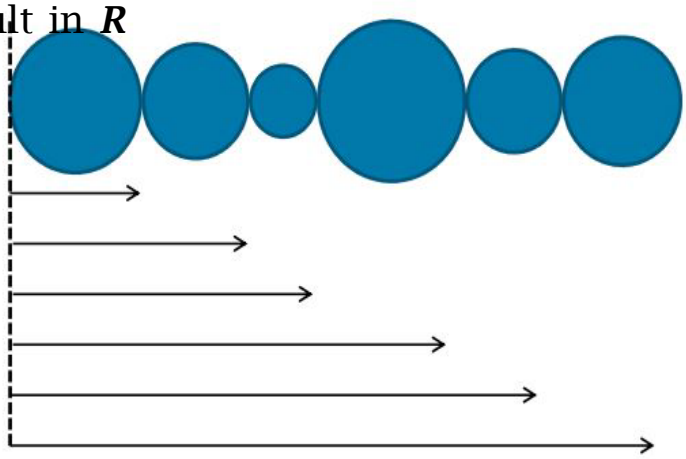

Normal Distribution $\frac{1}{\sigma\sqrt{2\pi}} e^{-\frac{(x-\mu)^2}{2\sigma^2}}$ $k \propto \frac{1}{x}$

Lognormal Distribution $\frac{1}{x\sqrt{2\pi\sigma^2}} e^{-\frac{(\ln x-\mu)^2}{2\sigma^2}}$ $k \propto \frac{1}{\ln(x)}$

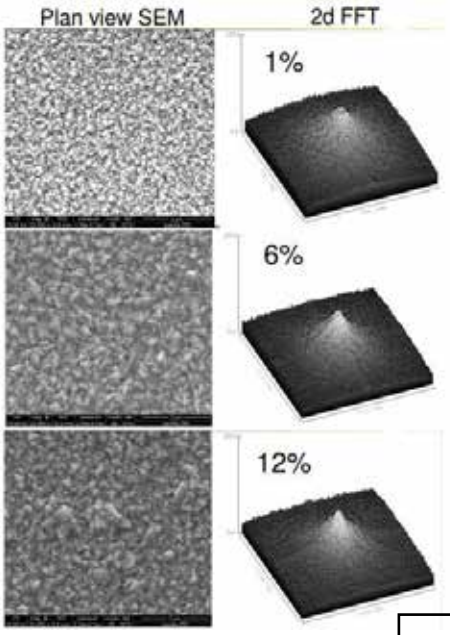

Grain Size Distribution Scales and is Lognormal

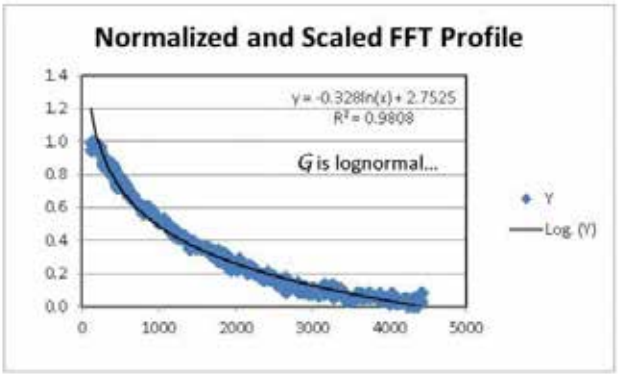

NANOXSOLAR
A division of IXS Technologies, Inc.

Materials and Design for Solar Applications

Optimization of Grain Size / Morphology Scattering amplitude vs. wave-length for different sizes of scattering features (SnO_2/Si interface)

Distribution of sizes (lognormal, σ=20% of μ)

For structures in Si, calculations indicate long length scale features should be ~$0.2_{\mu m}$

Red is high scattering Dark green is low scattering

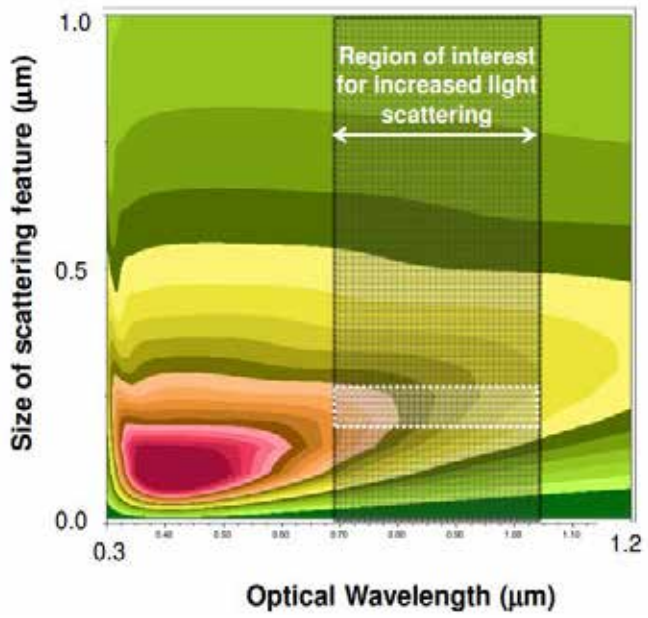

Device Performance with Buffer Layer

Device structure
- 50 nm CdS
- 850 nm CdTe

Process
- Magnetron sputtering
- Low substrate temp

Results
- HRT1
  - increased efficiency
  - increased process robustness

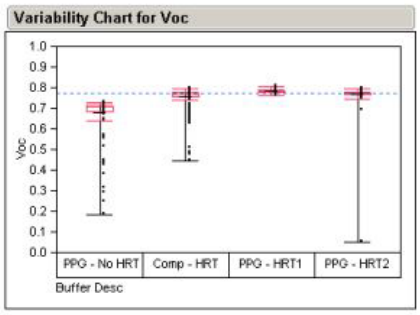

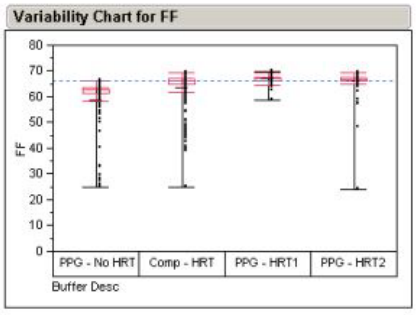

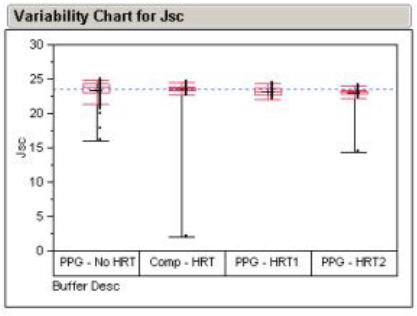

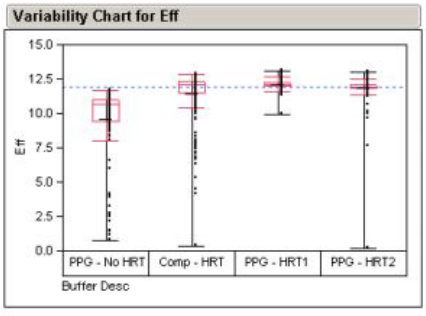

NANOXSOLAR
A division of IXS Technologies, Inc.

Transparent Fused Silica Types

Chart to Assist Memory

	Electric Melting	Flame Fusion	
Natural Quartz	Type I	Type II	Less Pure
Synthetic Precursors	Type IV	Type III	More Pure
	Dry	Wet	

Type III - Synthetic Fused Silica Vapor Phase Deposition

Flame Hydrolysis

Similar to flame fusion, except a silicon compound vapor (gas) is fed into the flame.
Chemical reaction generates a white soot.
Essential elements
- –Vapor source
- –Burner (hydrogen or methane with oxygen)
- –Substrate

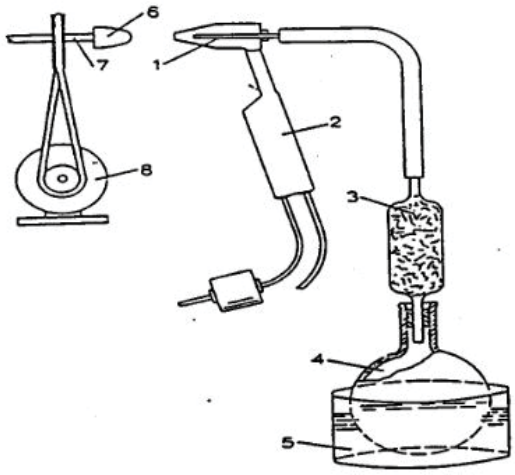

Figure 6. Flame Fusion of Synthetic Silica
1. Feed tube.
2. Oxy-hydrogen burner.
3. Filter tower.
4. Flask containing silicon compound.
5. Water bath.
6. Vitreous silica core.
7. Spindle.
8. Motor.

Synthetic Fused Silica Chemistry

Flame Hydrolysis
$SiCl_4 + 2H_2O = SiO_2$ (soot) + 4HCl (gas)

Vapor Phase Oxidation
$SiCl_4 + O_2 = SiO_2$ (soot) + $2Cl_2$ (gas)

–Both are oxidation processes.
–Hydrolysis dominates in hydrogen and hydrocarbon flame reactions.
–HCl and Cl_2 are not environmentally friendly by products

Type III - Synthetic Fused Silica Vapor Phase Deposition

Silica "Soot"

. Particle size about 100 nm with a total surface area greater than 20 m2/gm.

·If substrate is maintained above about 1800 ºC, simultaneous viscous sintering leads to a solid, bubble-free glass with a smooth surface.

·Substrate temperatures below about 1500 ºC lead to porous, partially sintered bodies that can be fully sintered (consolidated) in a subsequent step.

Soot Deposition

· Deposition rates greater than 1.5 gram/minute were achievable from a single burner in the 1970s, considerably more now.

· Can be scaled up by using multiple burners

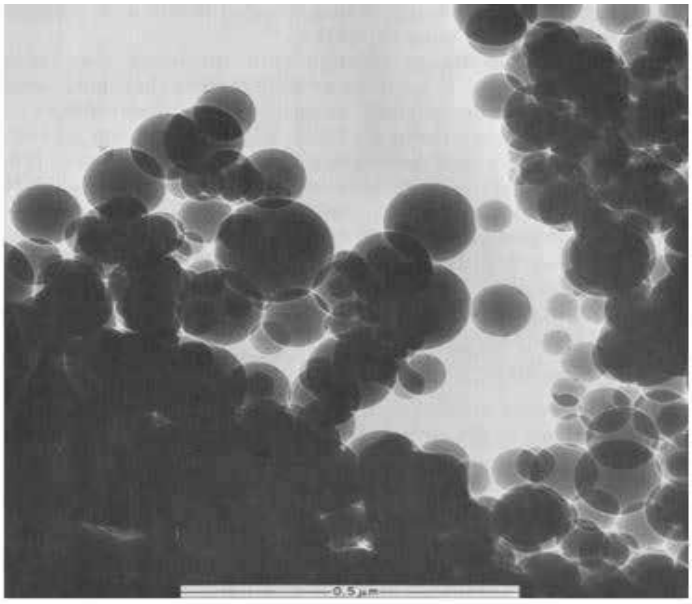

From Schultz and Scherer, 1983

Type III - Synthetic Fused Silica Vapor Phase Deposition

Corning 7940 and 7980 Process

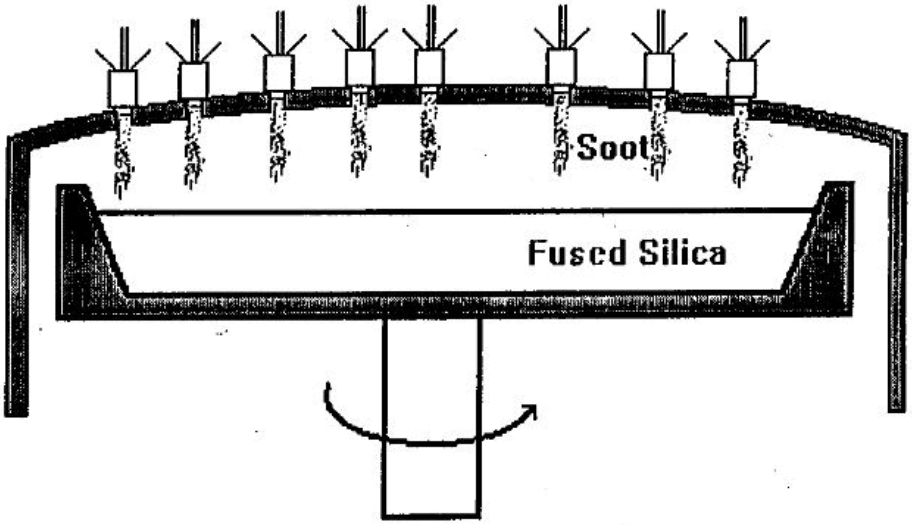

Courtesy of Corning Incorporated

Fused Silica Telescope Mirror

108"–diameter fused silica mirror blank made for a University of Texas astronomical telescope.

·Made by fusing together hexagonal blocks, each cut from individual boules (Hex-seal process), then boring the central hole, grinding and polishing.

·Note the outlines of the hexagons.

·Note also that once the blank is ground and polished to its final "figure," it will be coated with reflective aluminum, so the hex lines are of no consequence.

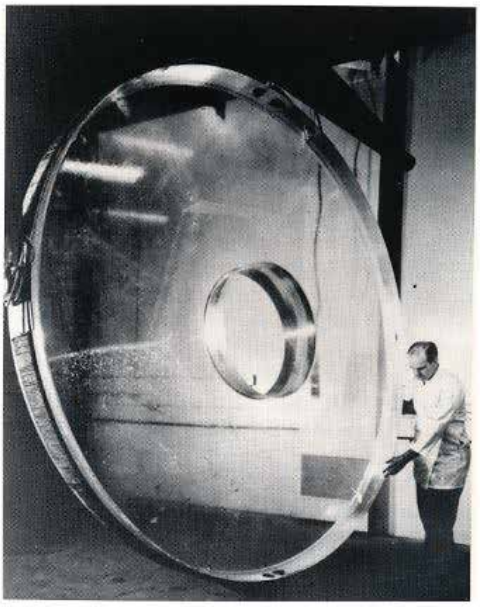

Corning Incorporated Product Literature

Type III - Synthetic Fused Silica Vapor Phase Deposition

Environmental Friendly Precursors

Environmentally more-friendly precursors - chain and cyclic siloxanes

–M.S. Dobbins and R.E. McLay (Corning) »U.S. Patent 5,043,002 (1991)
–I.G. Sayce, A. Smithson and P.J. Wells (Thermal Syndicate Ltd. / St. Gobain) British Patent 2,245,553 (1992)

Corning Code 7980 and Later Processes

Replaces SiCl4 by OMCTS

Combustion products
- SiO_2
- CO_2
- H_2O
- No Cl_2 or HCl

Environmentally friendly

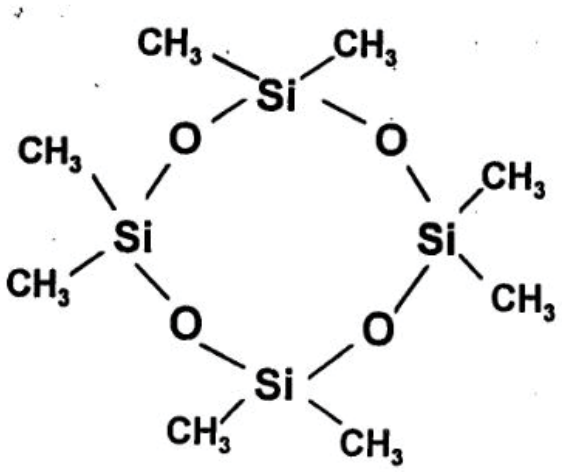

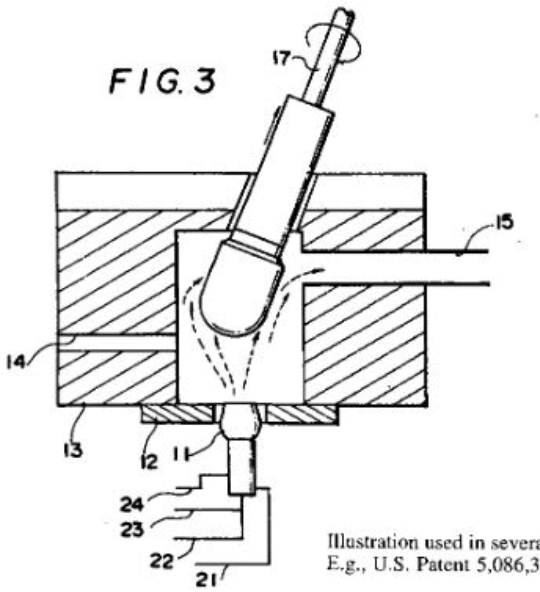

Illustration used in several Heraeus patents
E.g., U.S. Patent 5,086,352 (1992)

Heraeus Type III

·This is still a "boule" process, although the boules are considerably smaller than in Corning's 7980 process.

Type III - Synthetic Fused Silica Vapor Phase Deposition

Heraeus - Shin Etsu Type III

FIG. 4A

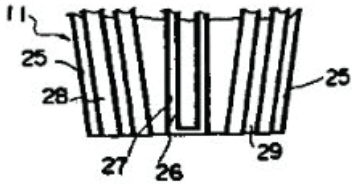

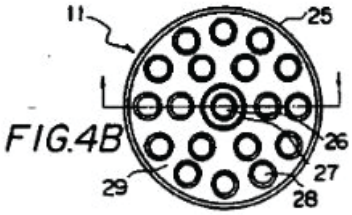

Burner Face Design

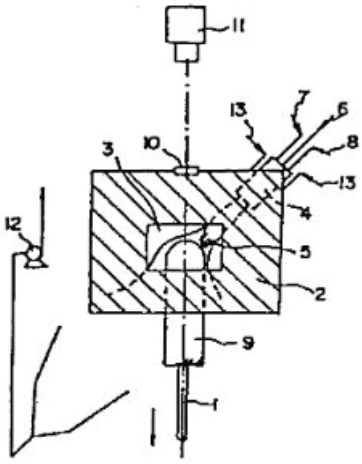

1. Heat-resistant support
2. Adiabatic material
3. Reaction chamber
4. Oxygen-hydrogen burner
5. Oxygen-hydrogen flame
6. Silicon compound
7. Oxygen gas supplying entrance
8. Hydrogen gas supplying entrance
9. Synthetic quartz glass rod
10. Viewing window
11. Radiation temperature gauge
12. Exhaust gas blower
13. Oxygen gas supplying entrance

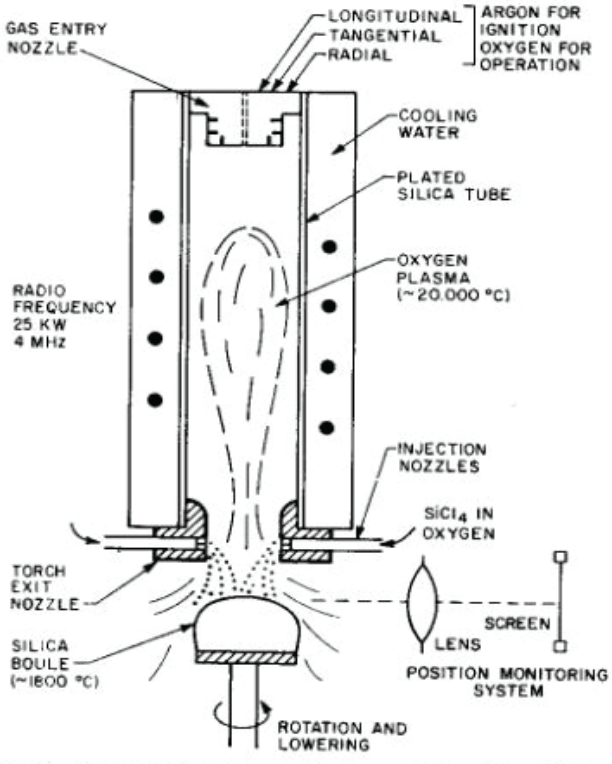

Fig. 2. Plasma torch arrangement for the production of fused SiO_2.

Plasma Torch

- A vapor phase oxidation process.
- Silica precursors enter in a dry (water vapor-free) gas stream.
- Again, a single-step boule process.
- Deposition rates greater than 0.5 gram/min are obtainable.

Two-Step Flame Hydrolysis (Soot Re-melting)

Synthetic - Two steps – Sometimes called “soot re-melting” process

–1 - Deposition of a porous preform (at temperatures too-low for viscous sintering) wherein all the pores are interconnected and open to the surface.
»Pore size is typically about 0.3 µm (300 nm)
»Porosity about 75%

–2- Drying and consolidating the preform under flow of gases
»Typically Cl, for drying
»And He or vacuum for rapid, pore free sintering

Very “Dry”- OH measured in ppm (< 10 ppm possible)

Very pure – metal ion impurities measured in ppm

Glass manufactured this way fits neither the Type III or Type IV category. I am arbitrarily calling it Type IVa.

Corning HPFS® Codes 7979 & 8655

This is a two-step soot re-melting process.

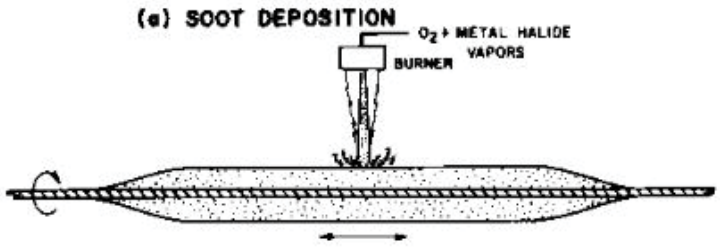

First, the soot is laid down as a mechanically stable, partially sintered porous body, on a rigid mandrel.

Second, the soot is dried and “consolidated” to full density in helium (rapidly diffusing gas) or vacuum atmosphere, with drying agents such as chlorine or carbon monoxide.

NANOXSOLAR
A division of IXS Technologies, Inc.

Two-Step Flame Hydrolysis (Soot Re-melting)

Shin-Etsu VAD · Shin Etsu (Japan), with Heraeus, has patented a process to conduct the two steps continuously, called Vapor Axial Deposition (VAD). · Again, a boule process.

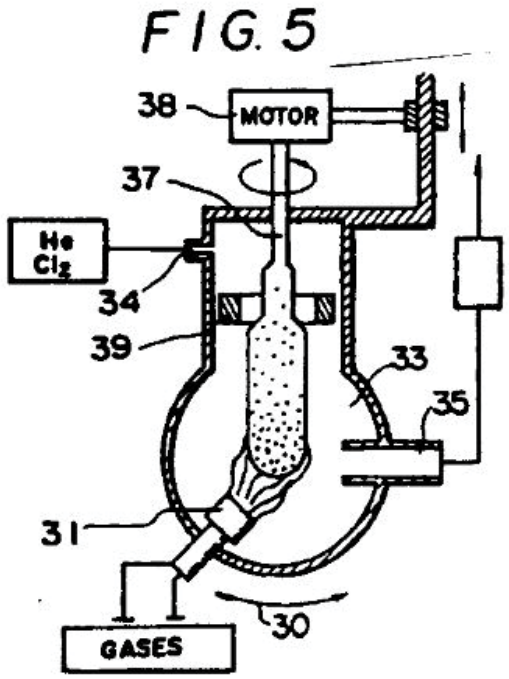

Change of Direction Adding Other Chemical Species to Synthetic Silica Glass

Doping of Fused Silica

Al_2O_3, ZrO_2, Nb_2O_5, Ta_2O_5, MoO_3, TiO_2, some 3d transition elements and a few others have been incorporated into Type III fused silica boules via this method. (Because of high vaporization rates, GeO_2, P_2O_5 and B_2O_3 are best added using the two-step process, Type IVa).

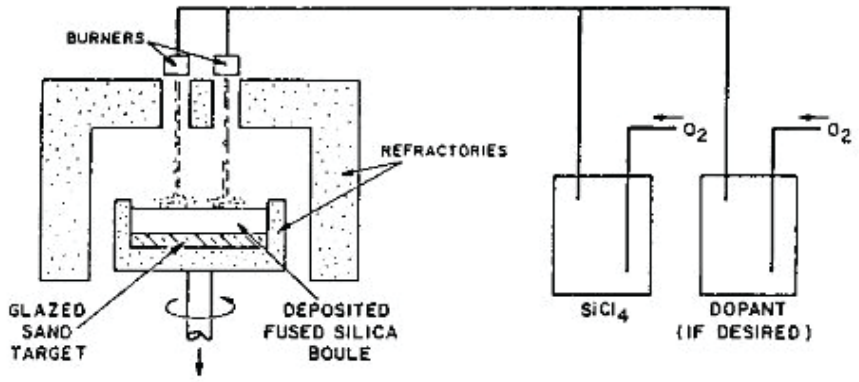

FIG. 10. Fused silica boule formed by simultaneous soot deposition and sintering in a flame oxidation furnace.

From Schultz and Scherer, 1983

ULETM Titania & Silica

Ultra-Low-Expansion ULETM(Corning Code 7971)
–TiO2 - doped fused silica (~ 7.5 wt% TiO2), TiCl4precursor.
–Made like synthetic fused silica Type III, one-step process.
–Much poorer UV transmission than pure silica.

Properties: Thermal expansion near zero from 5 ºC to 35 ºC, thus can be fusion sealed (welded) at room temperature enabling complex structures of extreme dimensional stability to be fabricated.

Note: Negative thermal expansion is observed at low temperatures, even for Corning Code 7940 fused silica.

NANOXSOLAR
A division of NXS Technologies, Inc.

Change of Direction Adding Other Chemical Species to Synthetic Silica Glass

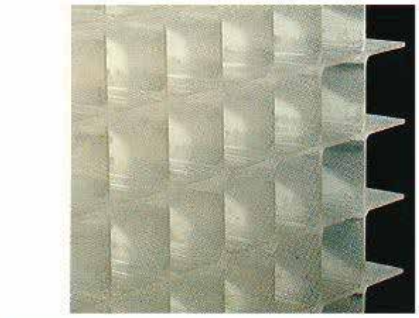

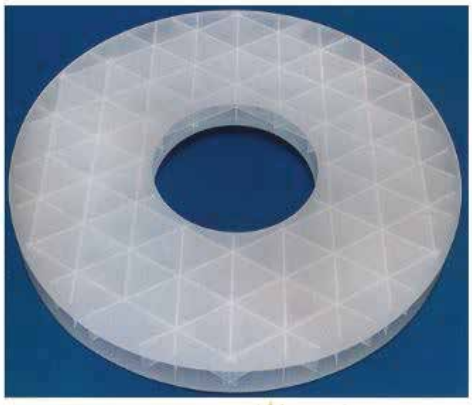

Fusion Sealing of ULETM

Corning Incorporated Product Literature

Low thermal expansion allows fusion sealing

(welding) of parts with negligible thermal shock. Complex, light-weight objects possible. ·Minimal annealing required.

Ultra Low Expansion ULETM (Corning Code 7971)

Hubble Space Telescope

Applications: telescope mirrors, light weight mirrors (for space), EUV microlithography stepper camera mirrors, precision athermal mountings and stages.

http://www.nanoxsolar.com/

Change of Direction Adding Other Chemical Species to Synthetic Silica Glass

Impregnation Method of Doping Preforms P.C. Schultz,

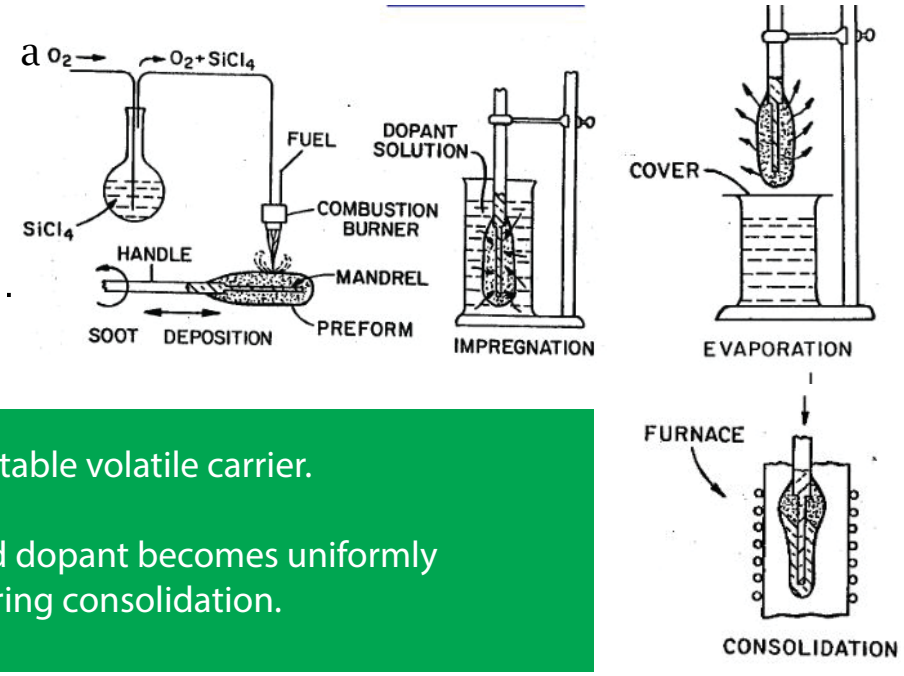

The dopant is dissolved in a suitable volatile carrier.

After evaporation the absorbed dopant becomes uniformly distributed within the glass during consolidation.

Diverse Silica Applications

Examples

-Earth- and space-based telescopes
-Space vehicle windows
-Microlithography stepper cameras and mirrors (for integrated circuit manufacture)
-Optical Communications Fiber

Reflecting Telescopes

Large Silica-based Optics: Earth-based telescopes

Need:
- –To see further into space
- –Study weaker signals

Mirror implications (theoretical):
- –Larger aperture (8meter diameter or greater or multiple mirrors)
- –Greater angular resolution
- –Shorter focal lengths; F/2 or less
- –Parabolic shape

Low thermal expansion

Low thermal mass (as important as low thermal expansion)

Other materials requirements:
- –Rigid, stable (no creep)
- –Capable of excellent polish (< 100 nm rms.)
- –Excellent chemical durability
- –Available in large sizes
- –Economically affordable

Recent Mirror Example Corning Incorporated

Size - 8 m class
Meniscus Type (mechanically supported thin mirror substrate)
Material - ULETM titania-doped silica
Hex-seal process, followed by thermal “sag” to shape

Example: Suburu (Japanese National Large) Telescope, Mauna Kea, Hawaii

Reflecting Telescopes

Glass Requirements for Microlithography Stepper Camera Lenses

Operating at 248 nm and 193 nm excimer laser wavelengths

Internal transmittance (through 1 cm glass at 193 nm) = 99%, preferred >99.5%

Refractive index homogeneity Δn < 2 x 10-6gradient < 0.1 x 10-6

Birefringence < 2 nm/cm

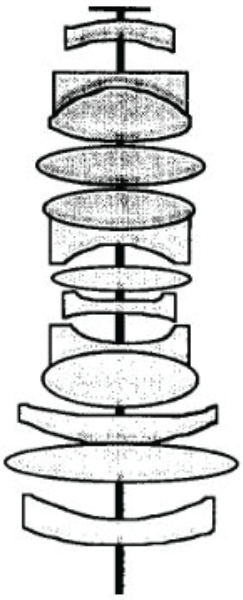

Example lens arrangement in stepper camera lens barrel

Stoichiometry and Impurity Defects

Non-Stoichiometry
–Oxygen excess or deficiency (network defects)

Dissolved molecular hydrogen (H2)
–Generally found in “wet” synthetic silica
–Conc. ~ 1017 to 1018 molecules/cm3

Dissolved chlorine
Important for understanding and controlling certain laser radiation-induced effects such as transmission loss (darkening) and dimensional changes (either compaction or swelling) during product use.

Need to minimize the compaction and swelling effects (ppm) prompted move from Type III to dry Type IVa glass for 193 nm lens applications.

Reflecting Telescopes

Glass Requirements for Microlithography Stepper Camera Mirror Optics

Need for faster microprocessors and more memory per chip requires smaller features on chip and shorter wavelength optics to produce them.

Industry is moving to EUV (extreme UV, wavelengths < 120 nm)
Transmissive optics (lenses) no longer workable; all oxide glasses are essentially opaque at these wavelengths.
Front surface mirrors are used for EUV
Excellent transmission is no longer important
But thermal expansion is.
Heating of mirror will change shape and distort image unless CTE is extremely small.
Therefore an important application for ULETM glass.

Optical Fiber for Telecommunications

VAD Process for Optical Fiber

– Vapor Axial Deposition

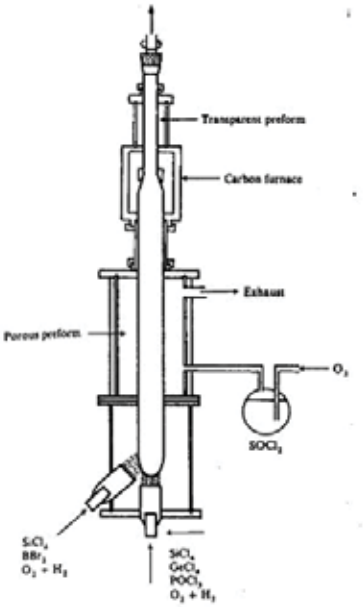

- Continuous process
- Soot deposited by two burners, each conveying a different combination of chemical streams to pro vide a refractive index gradient.
- Drying in separate chamber using flowing Cl2, SOCl2 or other gases.
- Consolidating at higher temperatures.

Key Innovation Dates

- Synthetic Fused Silica for Optical Fiber
First 20dB/km optical fiber (Corning)
- 1970

Outside process patented (Corning)
–D.B. Keck, P.C. Schultz & F. Zimar
»U.S. Patent 3,737,292 (1973)

Inside process (Corning)
–D.B. Keck & P.C. Schultz
»U.S. Patent 3,711,262 (1973)

Optical Fiber for Telecommunications

Corning OVD Process for Optical Fiber

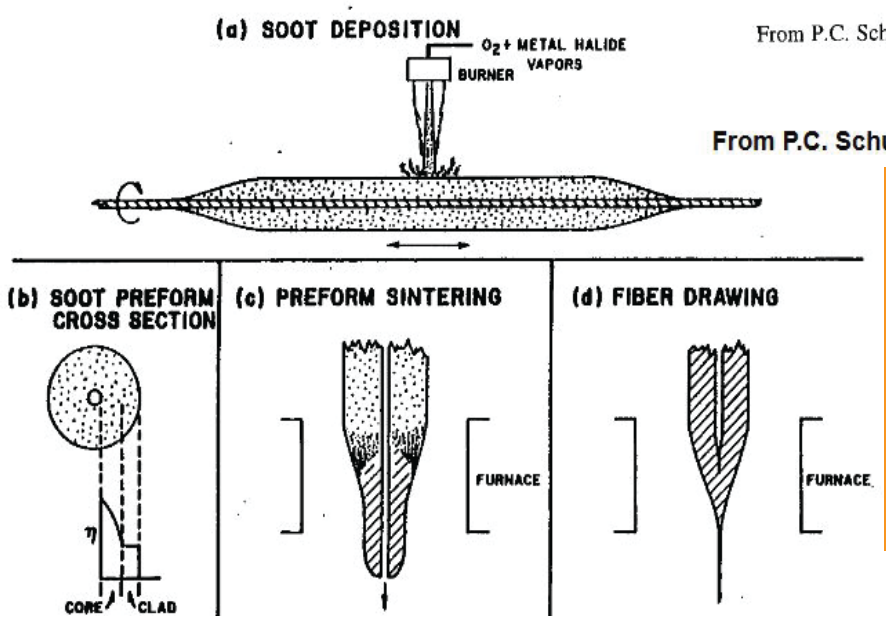

From P.C. Schultz

From P.C. Schultz, 1979

OVD – Outside Vapor Deposition Many layers (hundreds) deposited. Composition of vapor stream varied as a function of radius to provide the refractive index gradient.

IVPO / IVD Process for Optical Fiber

IVPO – Inside Vapor Phase Oxidation or IVD – Inside Vapor Deposition An oxidation process. No H2O produced in the reaction.

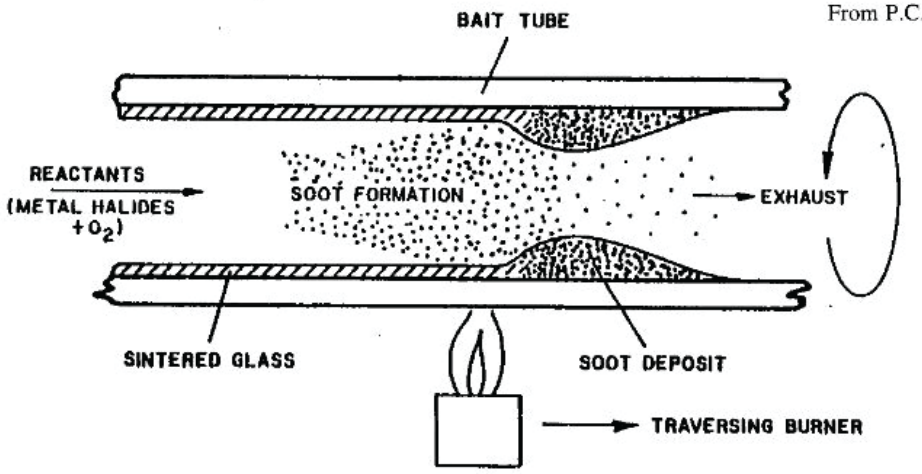

From P.C. Schultz

Figure 12. IVPO cross section.

From P.C. Schultz, 1979

SLIVER3000 Solar System Panel Specifications

Your Origin SLIVER system will be supplied with one of the following sets of panels:

Manufacturer	Mono Or Poly	Size (Watts)	Panels Required To Achieve Minimum 3000 Watts
SLIVER	Mono	150	20
SLIVER	Mono	157	20

The choice of panels will be at the sole discretion of our installer subject to such matters as stock availability.

Please see the following specification sheet for further details and panel specifications.

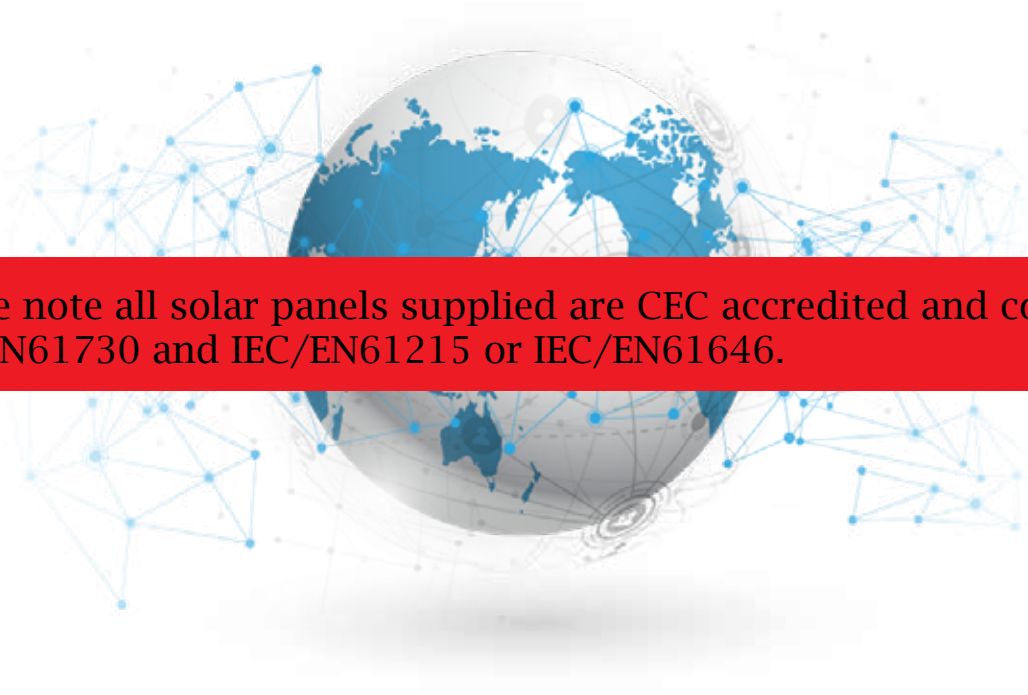

Please note all solar panels supplied are CEC accredited and compliant with IEC/EN61730 and IEC/EN61215 or IEC/EN61646.

NANOXSOLAR
A division of NXS Technologies, Inc.

High-Performance Series IV 150W Monocrystalline Silicon Photovoltaic

Our patented SLIVERTM technology, with 70 parallel connections per module, delivers near-linear partial shading response from the module and reduces system losses in common transient shade conditions regularly found on site.

Yield is increased by low operating temperatures and low temperature coefficients due to the unique cell architecture.

With triple interconnect redundancy and very low interconnect current in a cell, SLIVER modules deliver high reliability.

Our patented manufacturing process delivers distinctly different, ultra-thin monocrystalline and perfectly bifacial SLIVER cells.

Lower silicon consumption (g/W) enables faster energy payback time.

SLIVER modules' improved shade tolerance enables tighter row-to-row packing density, allowing array footprints to be minimized.

25-year warranty – See Transform Solar Limited Warranty for more details.

http://www.nanoxsolar.com/

Electrical Performance

SVR-HP150IV	STC[1] 1000 W/m²	NOCT[2] 800 W/m²
Maximum Power (Pmp)	150W	111.3W
Voltage @ Pmp	74.3V	68.4V
Current @ Pmp	2.02A	1.63A
Voltage Open-Circuit (V_{OC})	93.2V	87.3V
Current Short-Circuit (I_{SC})	2.27A	1.83A
Power Tolerance	±3%	–
NOCT Value	–	43°C
Temperature Coefficient Pmp	−0.41%/K	–
Temperature Coefficient I_{SC}	0.04%/K	–
Temperature Coefficient V_{OC}	−0.30%/K	–
Maximum System Voltage	600V	–
Maximum Series Fuse Rating	6A	–
Limiting Reverse Current	6A	–
Application Classification	Class A (IEC61730)	–

Note: Typical efficiency reduction @ 200 W/m² is less than 7%.
(1) Standard test conditions (STC) – 1000 W/m² irradiance, 25°C, and 1.5 air mass spectrum.
(2) Nominal operational cell temperature (NOCT) – 800 W/m² irradiance, 20°C ambient, and 1.5 air mass spectrum.

Mechanical Characteristics

SVR-HP150IV	
Dimensions (Length x width x depth)	1518 x 839 x 46mm (59.8 x 33.0 x 1.8in)
Weight	~17kg (~37.5 lbs)
Cell Type and Material	Monocrystalline silicon
Frame Material	Aluminum
Front Cover	3.2mm toughened glass
Encapsulant	EVA
Bypass Diode	1 per module
Junction Box Rating	IP67
Connectors	MC3- or MC4-compatible
PV Cable Length (each)	1000mm (39.4in)
PV Cable Area	2.5mm² (#14AWG)

SLIVER IV Curve (Typical)

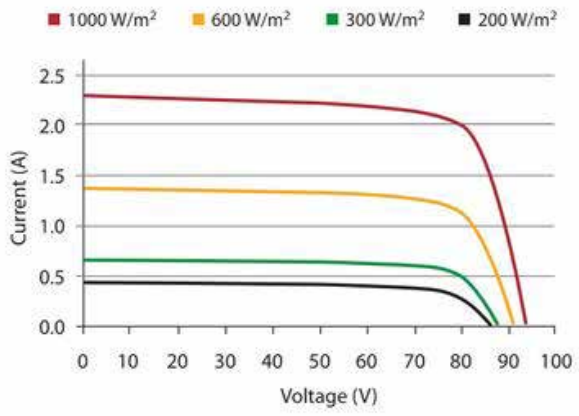

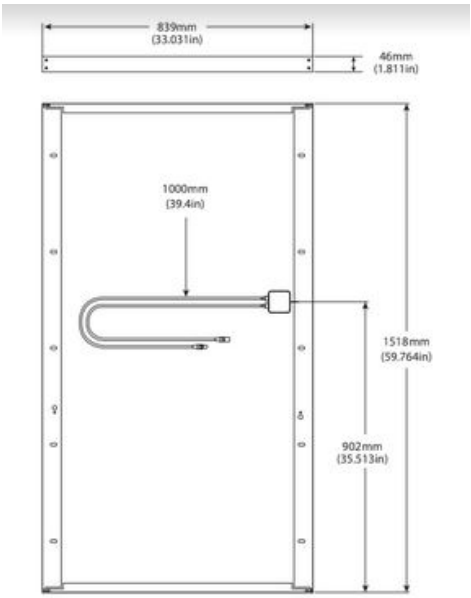

EResistively bounded subcells: A breakthrough for enhancing the performance of silicon solar

Introducing resistively bounded subcells: The lowest-cost method of increasing PV efficiency while improving safety and energy production

We are excited to introduce a breakthrough in the science of silicon photovoltaics, called Resistively Bounded Subcells (RBS). This new approach to photovoltaics requires no additional factory equipment or materials and it has sweeping applications across the solar industry.

- Mainstream panels and cells — more power, increased safety, reduced materials,and more lifetime energy production.
- Solar shingles for residential rooftops — tremendously simplified wiring and design, along with higher reliability
- Lanterns and solar home systems for low-income countries — higher voltage solar cells reduce electronics and complex module assembly
- Space applications — more flexibility in designing modules and more redundancy with fewer power electronics required
- Large format wafers — cells greater than 6 inches will benefit from reduced current loss due to electrical heat dissipation for elevated current flows
- Cell directly powers electronics without lossy voltage conversion (like cell phones or chargers).

Invented by Solar Invention's Chief Scientist, Dr. Benjamin Damiani, RBS creates multiple electrically isolated subcells on a single silicon wafer, using equipment and processes that already exist in most of the world's solar manufacturers. RBS works with 95% of all silicon cell architectures including monocrystalline, polycrystalline, PERC, HJT, and bi-facial. While scientists have long understood the idea of subcells (also called "monolithic cells"), creating them required specialized processing and was prohibitively limited in efficiency. Now, any manufacturer can immediately improve their profits,fabrication losses, and warranty returns — all without risk to throughput or quality.

First commercially available product — the Configurable Current Cell (C3)

The first commercially available product based on the RBS innovation is the Configurable Current Cell (C3). C3 reduces silver costs by 3% on the sunny side of a PV cell and up to 5% on the rear side of a PV cell, increases overall module power by 2-3 watts, and delivers higher lifetime energy in the field. In late 2019, the US Department of Energy recognized the promise of C3 by awarding Solar Inventions nearly $1 million as the first-ever recipient of the American Made Solar Prize.

For a 300-MW PERC cell and module manufacturer, C3 creates nearly US$1 million in value through this 3% reduction in silver and additional 2-3 watts per 60-cell panel. Because C3 strengthens the electrical divide for current inside a cell, heat-related issues are lowered, which reduces warranty claims and fire risks.

For cell manufacturers, C3 requires only small changes in metalization print patterns and selective doping. Manufacturers can implement C3 by working with Solar Inventions to modify their print screens and make a small set of additional easy and risk-free changes to their production lines. For modules, C3 configures the subcells in parallel to a cell's traditional busbars and therefore requires no changes to the tabbing and stringing of panels, making it quick and easy to introduce into an existing module manufacturer.

C3 mimics some of the benefits of split-cells and half-cells without the costs associated with physically cleaving the cells. C3 will power even more exciting applications as the industry continues increasing the size of cells. By subdividing the current in larger cells, C3 can reduce the resistive losses that increase as cell sizes grow past six inches.

First commercially available product — the Configurable Current Cell (C3)

Product roadmap — the Configurable Voltage Cell (CVC)

By connecting subcells in series within a single cell, the cell's voltage is increased proportionately. For example, a traditional cell might produce 0.65 volts at 9 amps, whereas a CVC cell with two subcells will produce 1.3 volts at 4.5 amps. This can be readily scaled up to any number of subcells — CVC has been successfully fabricated and tested with up to 12 subcells at UNC Charlotte and the Georgia Institute of Technology, generating more than 5 volts from a single, unbroken cell.

The applications of CVC are exciting and broad:

- Solar shingles with greatly simplified wiring requirements, greatly reducing the cost of residential solar
- Higher-voltage panels that can be wired in parallel, which simplifies inverter designs and reduces external power electronics
- Lower-cost single cells that directly power electronics, like phone chargers and solar lanterns for low-income countries.

CVC is still in laboratory development. Commercial pilots are anticipated for late 2020 or early 2021. C3 and CVC are complementary and can be used together, laying the foundation for rapidly commercializing a range of brand-new functionality and price- points in the solar marketplace.

First commercially available product — the Configurable Current Cell (C3)

The science behind Resistively Bounded Subcells

The patent-pending breakthrough behind C3 creates isolated changes in cell resistance.
This is done through a combination of metalization laydown changes and, in some cases, a post-metalization lasering step. Dr. Damiani's research has uncovered specific metalization patterns, both on the top and bottom of cells, that together create precise areas of higher cell resistance, which in turn are used as electrical boundaries around the hybrid subcells.

These subcells exhibit characteristics that have previously only been possible with exotic wafer processing techniques or physical cleaving such as half-cells.

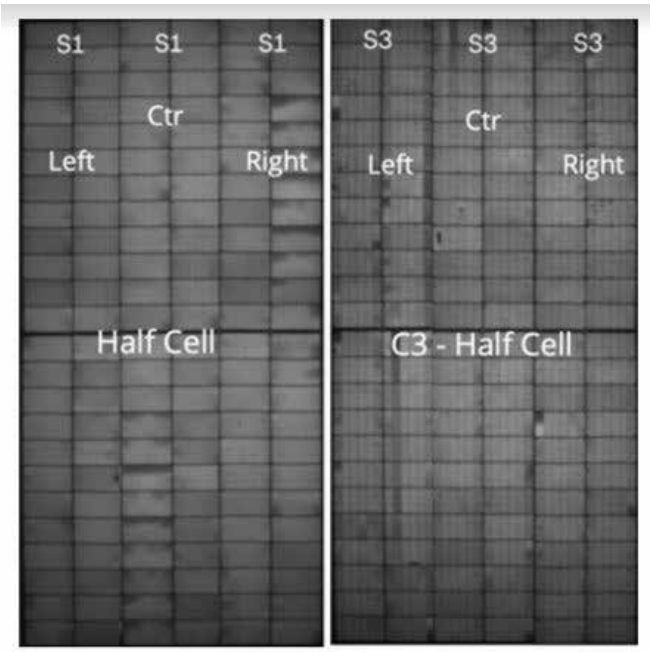

Figure 1. Electroluminescence image of a common half-cell module compared to a C3 enhanced half-cell module. Note the vertical segmentation for the C3 sample, which highlights the electrically isolated subcells.

C3 creates value across six areas:

1. Reduced metal consumption: 3%-5% reduction in silver

One of the most expensive components of fabricating a solar cell is the use of silver as electrical contacts on the front and/or rear side of a solar cell. The pattern used by C3 to create subcells results in a net silver savings proportional to the number of busbars on the cell. A three-busbar "H" pattern reduces silver consumption and and a six-busbar pattern reduces it further. See Figure 2 for a control chart of silver deposition during a sample pilot production of a five-busbar cell design. In certain cell architectures, the reduction in silver materials is matched by reduction in aluminum.

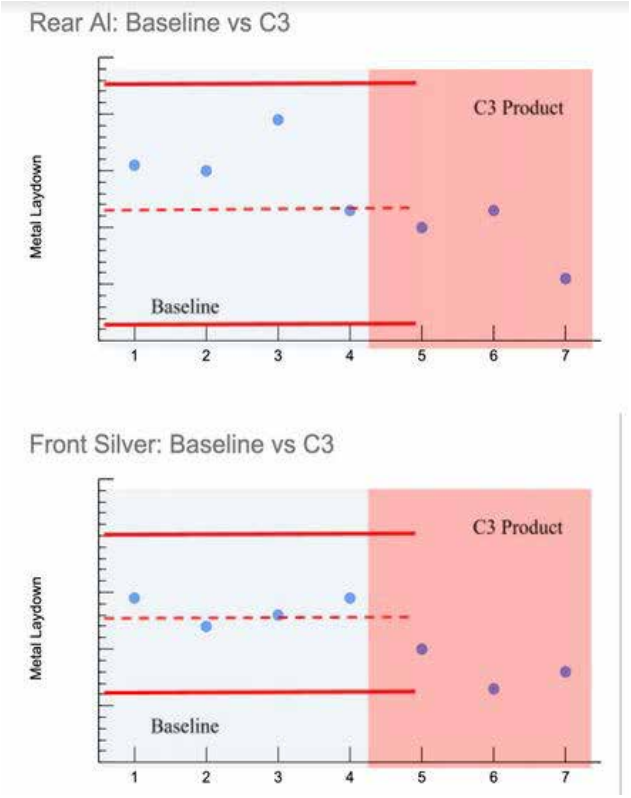

Figure 2. Process control chart measured during a 12-hour shift in a >500 MW solar cell fabrication plant, where the only change to production was a shift to C3 silver metalization on the front and rear side of the wafer. Both the front and rear side

C3 creates value across six areas:

2. Improved cell efficiency: 0.1%-0.2% absolute efficiency boost

The reduction in silver contact area acts to reduce the recombination velocity for metal on the silicon surface, resulting in a 1 mV-5 mV boost in open circuit voltage at the cell level. Figure 3 shows a data snapshot for C3 performance compared to the baseline group during the same production run for the silver savings shown in Figure 2.

The reduction in silver consumption also directly translates into less front metal shadowing, allowing more optical transmission into the bulk silicon for absorption and electrical current creation. Figure 4 shows the corresponding boost in short circuit current due to ~3% less front metal shadowing.

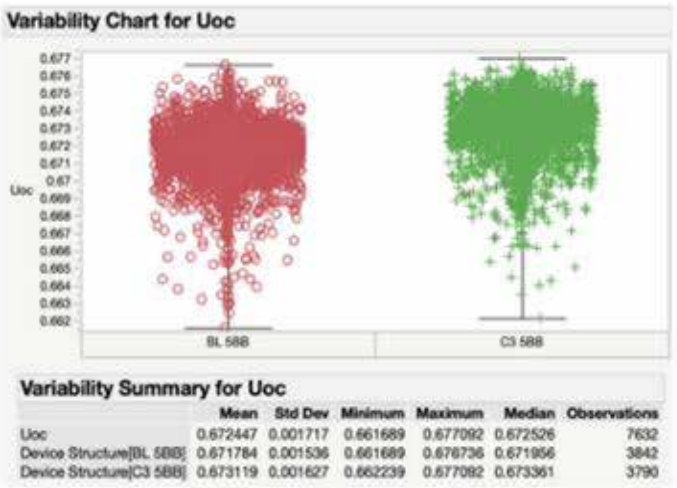

	Mean	Std Dev	Minimum	Maximum	Median	Observations
Uoc	0.672447	0.001717	0.661689	0.677092	0.672526	7632
Device Structure[BL 5BB]	0.671784	0.001536	0.661689	0.676736	0.671956	3842
Device Structure[C3 5BB]	0.673119	0.001627	0.662239	0.677092	0.673361	3790

Figure 3. Additional 1.3 mV of open circuit voltage for C3 enhanced mono PERC cells fabricated during the production run described in Figure 1.

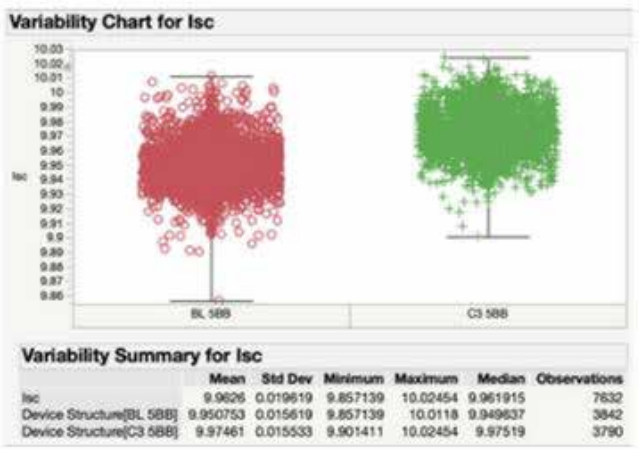

	Mean	Std Dev	Minimum	Maximum	Median	Observations
Isc	9.9626	0.019619	9.857139	10.02454	9.961915	7632
Device Structure[BL 5BB]	9.950753	0.015619	9.857139	10.0118	9.949637	3842
Device Structure[C3 5BB]	9.97461	0.015533	9.901411	10.02454	9.97519	3790

Figure 4. Additional 0.02 amps of short circuit current for C3 enhanced mono PERC cells fabricated during the production run described in Figure 1.

C3 creates value across six areas:

3. Improved Cell-to-Module Ratio (CTM)

The improved open-circuit voltage and higher short-circuit current results in higher module- level power because the module fill factor (FF) is unchanged compared with a standard PV cell, which in turn reduces CTM losses due to the higher open-circuit voltage (VOC) for the C3 enhanced modules. The CTM benefits require no changes to the existing stringing and encapsulation equipment. Figures 5 and 6 show module level data for the same production run referenced in this white paper. Taken together, the higher VOC in C3 modules combined with an unchanged FF raises the overall CTM and power output of a module. Similar results have been obtained from multiple mid- to large-scale module manufacturers.

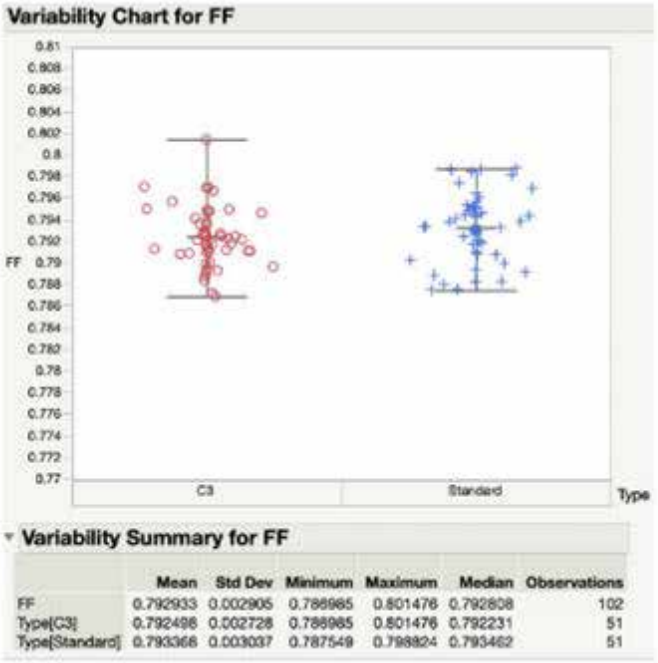

	Mean	Std Dev	Minimum	Maximum	Median	Observations
FF	0.792933	0.002905	0.786985	0.801476	0.792808	102
Type[C3]	0.792498	0.002728	0.786985	0.801476	0.792231	51
Type[Standard]	0.793368	0.003037	0.787549	0.798824	0.793462	51

Figure 5. Consistent fill factor for C3 enhanced mono PERC cells fabricated during the production run described in Figure 1.

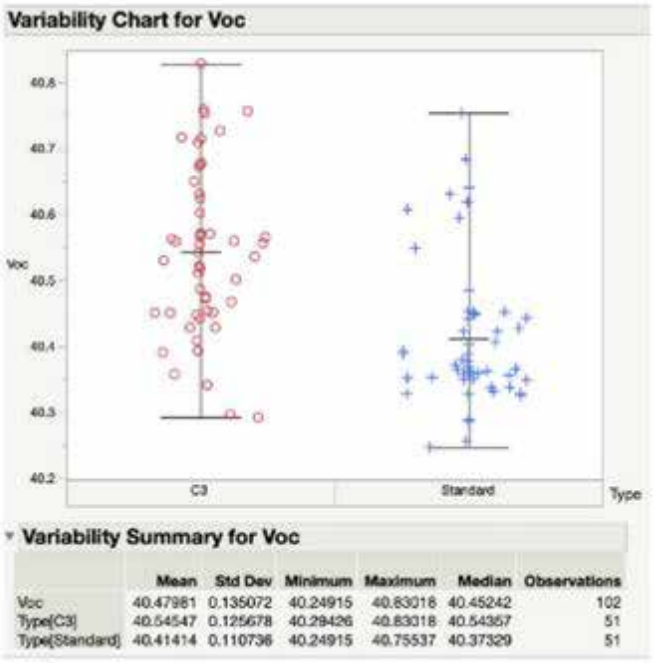

	Mean	Std Dev	Minimum	Maximum	Median	Observations
Voc	40.47981	0.135072	40.24915	40.83018	40.45242	102
Type[C3]	40.54547	0.125678	40.29426	40.83018	40.54357	51
Type[Standard]	40.41414	0.110736	40.24915	40.75537	40.37329	51

Figure 6. Increased open circuit voltage (~2mV per cell) for C3 enhanced mono PERC cells fabricated during the production run described in Figure 1.

C3 creates value across six areas:

4. Improved safety

The improved open-circuit voltage and higher short-circuit current results in higher module- level power because the module fill factor (FF) is unchanged compared with a standard PV cell, which in turn reduces CTM losses due to the higher open-circuit voltage (VOC) for the C3 enhanced modules. The CTM benefits require no changes to the existing stringing and encapsulation equipment. Figures 5 and 6 show module level data for the same production run referenced in this white paper. Taken together, the higher VOC in C3 modules combined with an unchanged FF raises the overall CTM and power output of a module. Similar results have been obtained from multiple mid- to large-scale module manufacturers.

The C3 electrical boundaries between each subcell slightly isolate the flow of current across the wafer, reducing current concentration around defects or small optical obstructions. The initial product release for C3 offers a mild improvement over baseline solar cells. Our next generation incorporates technology that substantially improves panel safety while decreasing power dissipation during a shading event.

5. Improved energy production compared to half-cells

The creation of subcells on a single silicon wafer without physically cleaving the solar cell maintains a smaller wafer perimeter compared to the wafer area of the individual solar cells. Each time a solar cell is cut in half, the ratio of the perimeter to the surface increases.

This results in non-ideal diode effects and higher edge recombination velocity for individual “Half Cells.” The C3 technology does not utilize a physical cleave and avoids the increased perimeter issue. Note that while C3 offers benefits over half-cells, it is entirely compatible with half-cells, offering improved power and safety benefits.

C3 creates value across six areas:

6. Reduced losses in large wafer sizes

The International Technology Roadmap for Photovoltaics (ITRPV) shows a trend toward larger wafer sizes. They are increasing past the standard 156mm, with factories starting to use wafers up to 210mm per square side. This increased size raises the cells overall short circuit current, but simultaneously increases the electrical heat loss (I^2R), reducing power. The most popular remedy is to cleave the cell into two or more physical pieces.

This requires expensive equipment upgrades,increased material losses, and reduced cell efficiency to contribute to module power. Subcells and the C3 technology allow an additional layer of flexibility that permits these increasingly larger formats to reduce their virtual size without the need for cleaving.

Solar startup wins $7.6 million in VC funding for innovative ribbon silicon furnaces

Leading Edge Equipment Technologies falls in the kerfless solar wafer or direct solar wafer category. According to the company, its "drop-in" manufacturing technology reduces wafer costs by 50%, increases commercial solar panel power by up to 7%, and reduces manufacturing emissions by over 50%. It's the emissions piece that might be winning over investors.

Leading Edge Equipment Technologies, a startup making manufacturing equipment to produce kerfless, single-crystal silicon wafers for solar panels, just closed on a $7.6 million series A financing. The round was led by Prime Impact Fund, Clean Energy Ventures along with DSM Venturing. Previous investors in the startup include Applied Materials, Clean Energy Venture Group and David Buzby.

The company's technology falls in the kerfless wafer or direct-wafer category. Kerfless production does not require silicon ingots to be sawn into wafers, a time- and energy-consuming multi-step process which uses consumables and wastes material as silicon dust.

According to the company, its "drop-in" manufacturing technology reduces wafer costs by 50%, increases commercial solar panel power by up to 7%, and reduces manufacturing emissions by over 50%.

Rick Schwerdtfeger joined Leading Edge as CEO and Nathan Stoddard joined as CTO earlier this year. Prior to this funding round, the startup received $1.45 million in angel and venture funding, according to Pitchbook, and has received $4 million in DOE funding. Founder and board member Alison Greenlee, with previous experience at kerfless silicon wafer startup 1366 Technologies, is chief product officer.

Ribbon solar

The company's product is a new type of silicon wafer production furnace.
cally a net shape wafer coming out of the furnace."

Solar startup wins $7.6 million in VC funding for innovative ribbon silicon furnaces

> *"The furnace is actually producing a single crystal — basically a one-wafer-wide ribbon that comes out of the furnace, and then is laser cut at the furnace into sections, and those sections can be further laser-cut or cleaved into net shape wafers with no need for diamond sawing and saw damage removal etching — and no need for the traditional cropping and all the challenges of taking a very large CZ boule and turning it into thin wafers. We grow basically a net shape wafer coming out of the furnace."*

CEO Rick Schwerdtfeger told pv magazine,

The "*Floating Silicon Method*" process was pioneered by Leading Edge founder Peter Kellerman while at Varian Semiconductor, which was later acquired by Applied Materials for $4.9 billion back in 2011. Silicon solar's dirty little secret

Schwerdtfeger, the CEO, said the "*dirty little secret*" of solar power was the energy intensity and emissions in the purification and forming of the silicon materials. He said, "Our process wastes virtually no silicon — and that has a major impact on factory emissions."

That emissions component cited by the startup is of increasing importance to investors with an ESG thesis and one that the Ultra Low-Carbon Solar Alliance is attempting to address. The alliance looks to grow market awareness around solar supply chain decarbonization.

http://www.nanoxsolar.com/

Solar startup wins $7.6 million in VC funding for innovative ribbon silicon furnaces

Other startups have gone down the kerf-less road and met with limited success. Twin Creeks and SiGen attempted to manufacture kerfless silicon using ion-implantation. Crystal Solar and Ampulse were working gas-to-wafer technology. Evergreen Solar was a publicly-listed ribbon solar company. These firms are defunct.

1366 Technologies is still alive and forming wafers directly using molten silicon.

Leading Edge's customers are the solar module incumbents and perhaps some hungry upstarts challenging those incumbents. The startup CEO said he looks to have "furnaces into the field by late next year."

Schwerdtfeger told pv magazine that the reason he took this job was because "This is the most disruptive innovation I've seen in silicon in the last 30 years — and I have to be part of it."

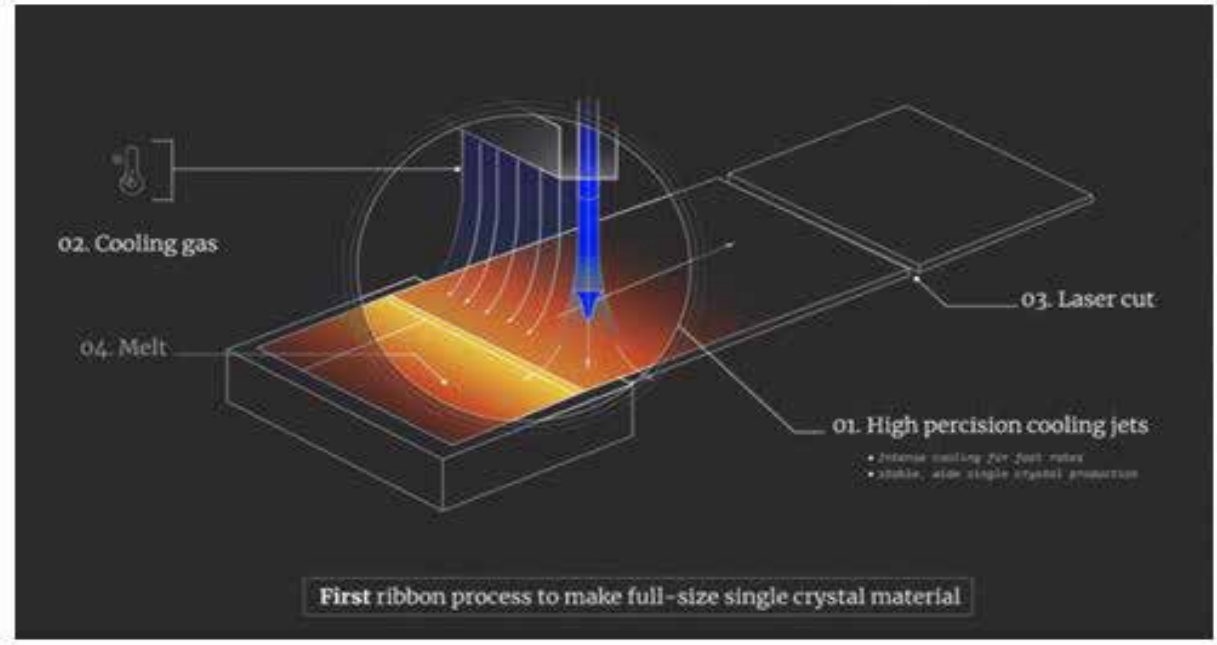

Gigawatt-scale tandem solar cell production by 2022? Would you take that bet?

1366 Technologies CEO Frank van Mierlo is a betting man and he's betting your humble narrator that high-efficiency tandem solar cells are the near-term commercial future of solar.

November 5, 2020 Eric Wesoff

Frank van Mierlo, the CEO of 1366 Technologies, is a betting man — and he's wagering that "the solar market will see 2 GW of tandem solar in the marketplace by the end of 2022."

I am the skeptic on the other side of this wager for one bottle of fine champagne — although I would accept a thimbleful of the CEO's tears in its place.

van Mierlo, chief of a kerfless silicon wafer startup, has said: "*I've never doubted silicon. We really believed in it. The learning curve had been holding steady for 45 years – it's a pretty predicable line. Why would that stop?*"

So, when we heard van Mierlo at a recent talk saying that tandem modules made from a high-bandgap and a low-bandgap material are "*the most important innovation in solar since solar was first conceived in Bell Labs in 1954*," it seemed that 1366 was pivoting to a new technology and approach.

van Mierlo makes the case When I asked van Mierlo about this seeming shift to tandem, and voiced my concern with this technology path, the CEO suggested we embark on a small wager about tandem's commercial future.

He believes that the solar market will see 2 GW of tandem solar in the marketplace by the end of 2022.

Gigawatt-scale tandem solar cell production by 2022? Would you take that bet?

van Mierlo writes, "I*n fact, not only do I believe that multiple gigawatts of tandem will be sold before the end of 2022, I am also confident that in a decade's time, tandem will command more than 50% of our industry's market share.*"

He continues: "*Is it that I no longer believe in the long-term role of silicon?*"

"No! In fact, it's the remarkable success of silicon that now makes tandem modules the inevitable next step. With its low bandgap of 1.1 eV and its low cost, silicon is the ideal candidate for the bottom cell in a tandem configuration. In this position, a silicon bottom cell converts less than one-third the energy captured by the sun but still carries 100% of the cell cost. To make tandem work, you need the bottom cell to be extremely low cost. And, thanks to recent innovations such as the Direct Wafer furnace, we can achieve that cost target.

It is precisely because of silicon's dramatic learning curve that tandem will soon be a commercial reality. As module costs have declined and many installation costs remain fixed, we've witnessed the increased pressure for greater efficiency. This pressure will drive tandem adoption: its dramatic efficiency boost without a significant increase in module cost-per-watt will lower the installed cost of solar by producing more power for a given area.

"We know that the headroom for increasing efficiency with single-junction silicon technology is closing. It is the opportune moment for tandem modules underpinned by extremely low-cost silicon."

Which brings us to the tandem top cell, for which there are many excellent solutions. Thanks to the massive investment in thin film R&D, there are suitable materials already on the shelf. Moreover, new perovskites bring additional promise.

Oxford PV and Swift Solar both vouch that it is possible to make a stable high-bandgap perovskite, but it is much harder for perovskites to match the excellent low-bandgap performance of silicon.

Gigawatt-scale tandem solar cell production by 2022? Would you take that bet?

"*Silicon's next contribution will be to tandem as an extremely low-cost and high-performing bottom cell.*"

"*I am looking forward to drinking that champagne*," taunted the CEO.

Tandem solar startups

Since its founding, 1366's technology has been based on forming solar wafers directly, using molten silicon, instead of silicon ingots sawn into wafers. Over the last 14 years, 1366 has raised more than $100 million from investors including Breakthrough Energy Ventures, Tokuyama, North Bridge, Polaris, VantagePoint, Energy Technology Ventures, Hanwha Chemical, Ventizz Capital and Haiyin Capital.

Tandem structures can be epitaxially grown monolithically on silicon or mechanically stacked. The tandem-junction cell architectures have potential efficiency gains because of the different wavelength ranges and bandgaps of silicon and other materials.

Tandem solar startups include:

Oxford PV has raised more than $140 million to develop perovskite-on-silicon tandem solar cells and modules. Meyer Burger has partnered with the startup to develop equipment and has also taken an equity stake in the firm.

Swift Solar stacks perovskite solar cells to make tandem cells. The company can put these layers on flexible substrates and foils.

Tandem PV aims to monolithically print thin-film perovskites on a glass panel and mechanically stack it on top of silicon cells.

Other perovskite solar technology developers include Saule Technology and HPT.

I win this bet

As we've reported, commercial crystalline silicon is forecast to reach efficiencies of 22%-24% by the end of the decade, and possibly 25% if interdigitated back-contact (IBC) heterojunction products get to market.

Gigawatt-scale tandem solar cell production by 2022? Would you take that bet?

NREL studies find that reaching cost reductions in photovoltaics beyond the 6¢/kWh SunShot 2020 goal will mean that cell efficiency must be increased beyond the Shockley–Queisser limit of 29.4% for a single p-n junction. Other researchers have found that PV modules made with tandem solar cells will have to show efficiencies of 30% and offer the same lifetime and degradation rate as standard crystalline panels if manufacturers want to hit commercial production.

That said, I win this bet because:

Reliability: Silicon is the most studied element in the periodic table, and the globe will deploy more than 100 GW of the stuff in PV applications this year. We know its failure modes and its long term behavior. Other potential tandem materials such as perovskites or CIGS exhibit different and relatively unstudied failure modes and degradation paths. It will take years to gain confidence in the long-term reliability of a new materials system or tandem combination. Even if we understand each materials system separately — what happens when they are mingled in these 30-year assets in increasingly hostile environments?

Developers, banks, underwriters: A solar project is an investment tool that turns photons into kilowatt-hours and dollars — and the extremely risk-adverse financial community does not tolerate new, unproven technologies. Greater risk in any aspect of a solar project translates to nervous underwriters, a higher cost of capital and an uncompetitive project.

History is on my side: The road is littered with the remains of hundreds of solar aspirants, all keen to commercialize some alternative to straight-up crystalline silicon — amorphous silicon, CIGS, CdTe, or GaAs. Not one company, other than First Solar, has been able to succeed commercially in this effort.

Time is on my side: Yes, it is.

I will toast your health with my victory champagne in Dec 2022.